TABLE 1. Macaques used in this study

Group	Animal identification codes	Vaccination[a]
I	R02-007, R06-037, R07-001, R07-004, R07-009, R06-019	None
II	R02-008, R05-026, R06-004, R06-014, R06-040, R07-006	Control vaccination [pEGFP-N1 DNA prime, F(−)SeV-EGFP boost]
III	R04-016, R06-007, R07-002, R07-003, R07-007, R07-008	$Gag_{241-249}$-specific vaccination [p$Gag_{236-250}$-EGFP-N1 DNA prime, F[(−)SeV-$Gag_{236-250}$-EGFP boost]

[a] All animals were challenged with SIVmac239.

nasal boost with the F(−)SeV-$Gag_{236-250}$-EGFP vector. Group II animals were administered pEGFP-N1 DNA and the F(−)SeV-EGFP vector, both expressing EGFP instead of $Gag_{236-250}$-EGFP, as a control vaccine.

We measured the antigen-specific $CD8^+$ T-cell responses in these macaques 1 or 2 weeks after the SeV boost by detection of specific IFN-γ induction. All group III macaques showed efficient $Gag_{241-249}$-specific $CD8^+$ T-cell induction after the F(−)SeV-$Gag_{236-250}$-EGFP boost (Fig. 1B). In these animals, we also confirmed SeV-EGFP-specific $CD8^+$ and $CD4^+$ T-cell responses (Fig. 1C) but did not detect $Gag_{206-216}$-specific $CD8^+$ T-cell responses, which are dominantly induced in *90-120-Ia*-positive macaques by Gag-expressing SeV vaccination (14). We have never found $Gag_{236-250}$-specific $CD4^+$ T-cell responses in any previously examined animals, and as expected, analyses with the $Gag_{236-250}$ peptide did not detect $Gag_{236-250}$-specific $CD4^+$ T-cell responses in any of the group III animals in the present study. In group II animals, we detected SeV-EGFP-specific T-cell responses but not $Gag_{236-250}$-specific T-cell responses after the F(−)SeV-EGFP boost (data not shown).

Control of an SIV challenge in vaccinees. Group I (unvaccinated), II (control-vaccinated), and III ($Gag_{236-250}$-vaccinated) macaques were challenged intravenously with SIVmac239. Plasma viral loads in these animals were examined after the challenge (Fig. 2A). Most of the group I and II animals failed to contain SIV replication, although plasma viremia became undetectable at week 12 in one animal in group I (R06-037) and one in group II (R06-004). No significant differences were observed between groups I and II in plasma viral loads at the peak, at week 5, at week 12, or around week 24 after the challenge. In contrast, most group III animals contained SIV replication; plasma viral loads became undetectable after week 5 in five of the six animals (Fig. 2A). Plasma viral loads in these animals were significantly lower than those in unvaccinated group I and those in control-vaccinated group II at the peak, at week 5, and at the set point (Fig. 2B). Thus, the prophylactic vaccination inducing $Gag_{241-249}$ single-epitope-specific $CD8^+$ T-cell responses resulted in a significant reduction of peak and subsequent viral loads after the SIV challenge. No significant difference in peripheral $CD4^+$ T-cell counts was observed among these three groups (Fig. 2C).

Dominant $Gag_{241-249}$-specific $CD8^+$ T-cell responses in vaccinees after a SIV challenge. We assessed virus-specific $CD8^+$ T-cell responses at weeks 2 and 12 after a SIV challenge by measuring antigen-specific IFN-γ induction. $Gag_{241-249}$-specific $CD8^+$ T-cell responses were undetectable or marginal in some naive controls (group I and II) but were efficiently induced in all of the group III animals (Fig. 3A). In most of the naive controls, $Gag_{206-216}$-specific $CD8^+$ T-cell responses were induced equivalently or more efficiently than $Gag_{241-249}$-specific $CD8^+$ responses, whereas all of the group III animals showed dominant induction of $Gag_{241-249}$-specific $CD8^+$ T-cell responses. In these group III animals, $Gag_{206-216}$-specific $CD8^+$ T-cell responses were inefficient but frequencies of $CD8^+$ T cells exhibiting $Gag_{241-249}$-specific IFN-γ induction were significantly higher than in naive controls at week 2 (Fig. 3B) and week 12. $Gag_{241-249}$-specific $CD8^+$ T-cell frequencies at week 2 inversely correlated with peak viral loads (Fig. 3C).

We also tested SIV-specific $CD8^+$ T-cell responses in these animals (Fig. 4). We used *env* and *nef* deletion-containing simian-human immunodeficiency virus molecular clone DNA SIVGP1 containing the genes encoding SIVmac239 Gag, Pol, Vif, Vpx, and a part of Vpr and measured the frequencies of $CD8^+$ T cells responding to SIVGP1-transduced cells (referred to as SIV-specific $CD8^+$ T cells) as described previously (15). Naive controls (groups I and II) and vaccinees (group III) were found to possess similar levels of SIV-specific $CD8^+$ T cells at week 2 and week 12.

In our previous study (27), all of the *90-120-Ia*-positive macaques vaccinated with Gag-expressing SeV contained SIV replication with rapid selection of a *gag* mutation (GagL216S), resulting in escape from $Gag_{206-216}$-specific $CD8^+$ T-cell recognition at week 5, implicating $Gag_{206-216}$-specific $CD8^+$ T-cell responses (rather than $Gag_{241-249}$-specific $CD8^+$ T-cell responses) in viral control. In the present study, however, five of six $Gag_{236-250}$-vaccinated animals controlled SIV replication and had undetectable set point viremia without selection of *gag* mutation over 5 weeks (data not shown). No *gag* mutation was selected at week 5 in naive controls, either. These results indicate that in the group III macaques, dominantly induced $Gag_{241-249}$-specific $CD8^+$ T-cell responses in the acute phase play an important role in this vaccine-based SIV control.

Higher $Gag_{241-249}$-specific effector memory $CD8^+$ T-cell frequencies in vaccinees. We then examined $Gag_{241-249}$-specific $CD8^+$ T-cell frequencies in these macaques by using PE-conjugated $Gag_{241-249}$-A*90120-5 tetramers. In group III animals, $Gag_{241-249}$-specific tetramer$^+$ $CD8^+$ T cells were still detectable just before the SIV challenge, and their frequencies increased greatly after the challenge; most of the vaccinees exhibited a >10-fold increase at week 2 compared to prechallenge levels (Fig. 5A). Increases in tetramer$^+$ $CD28^-$ $CD8^+$ T-cell frequencies after a challenge were especially marked (>30-fold) (Fig. 5B). Indeed, within the tetramer$^+$ cells, the ratio of $CD28^-$ cells increased after a challenge and these cells became predominant at week 2. Analysis of an effector memory subset delineated by the $CD95^+$ $CD28^-$ phenotype (29, 34) revealed significantly higher frequencies of $Gag_{241-249}$-specific tetramer$^+$ $CD95^+$ $CD28^-$ $CD8^+$ T cells in group III than in naive controls (Fig. 5C). These results suggest efficient responses of $Gag_{241-249}$-specific $CD8^+$ T cells with effector function in the acute phase in group III animals.

$Gag_{241-249}$-specific cytolytic $CD8^+$ T-cell responses in vaccinees. To further investigate the cytolytic quality of $Gag_{241-249}$-specific $CD8^+$ T-cell responses after a challenge, we examined

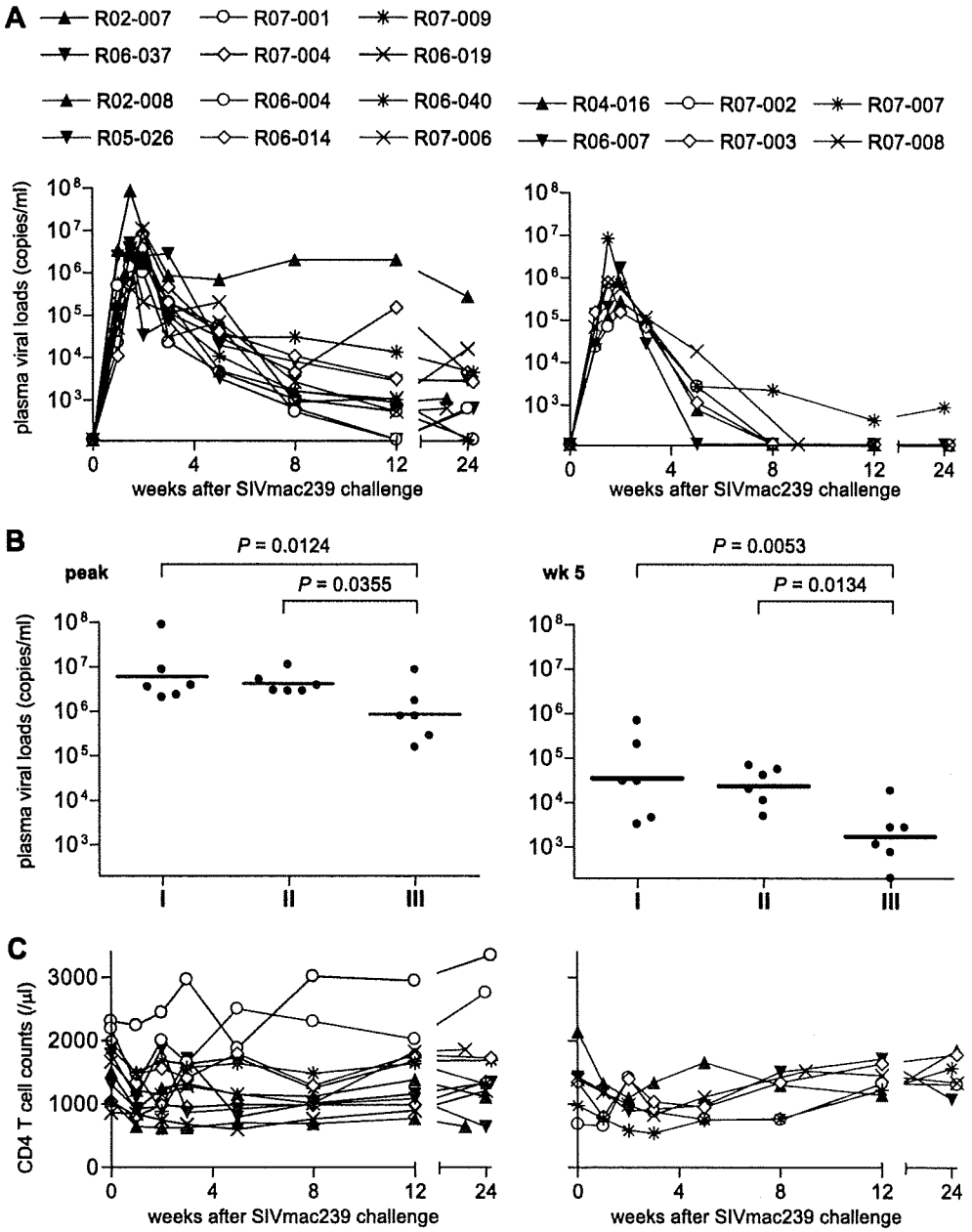

FIG. 2. Plasma viral loads and peripheral CD4$^+$ T-cell counts after a SIV challenge. (A) Changes in plasma viral loads (SIV *gag* RNA copies/ml plasma) in unvaccinated group I animals (black lines in the left panel), control-vaccinated group II animals (blue lines in the left panel), and $Gag_{236\text{-}250}$-vaccinated group III animals (red lines in the right panel) after a SIVmac239 challenge. Plasma viral loads were determined as described previously (27). The lower limit of detection is approximately 4×10^2 copies/ml. (B) Comparisons of plasma viral loads in groups I ($n = 6$), II ($n = 6$), and III ($n = 6$) at the peak (left panel) and at week 5 (right panel). The bar indicates the geometric mean of each group. Viral loads at the peak and at week 5 in group III were significantly lower than in group I ($P = 0.0124$ at the peak and $P = 0.0053$ at week 5) and group II ($P = 0.0355$ at the peak and $P = 0.0134$ at week 5). There were no significant differences between groups I and II either at the peak or at week 5 ($P = 0.6047$ at the peak and $P = 0.6536$ at week 5). Set point viral loads in group III were significantly lower than those in group I and group II at week 12 by nonparametric analysis ($P = 0.3939$ between I and II, $P = 0.0152$ between I and III, and $P = 0.0152$ between II and III; $P = 0.1797$ between I and II, $P = 0.0260$ between I and III, and $P = 0.0411$ between II and III around week 24). (C) Changes in peripheral CD4$^+$ T-cell counts (per μl) in groups I (black lines) and II (blue lines) in the left panel and in group III (red lines) in the right panel after a SIVmac239 challenge.

$Gag_{241\text{-}249}$-specific induction of CD107a (a degranulation marker), which is related to cytolytic activity (21, 38), in CD8$^+$ T cells at week 2. Frequencies of CD8$^+$ T cells exhibiting $Gag_{241\text{-}249}$-specific induction of CD107a, as well as IFN-γ, within the CD8$^+$ T-cell pool were significantly higher in group III than in naive controls ($P = 0.0249$ by unpaired t test) (Fig. 6). One animal, R04-016, in group III did not show $Gag_{241\text{-}249}$-specific CD107a$^+$ IFN-γ$^+$ CD8$^+$ T-cell responses, but further

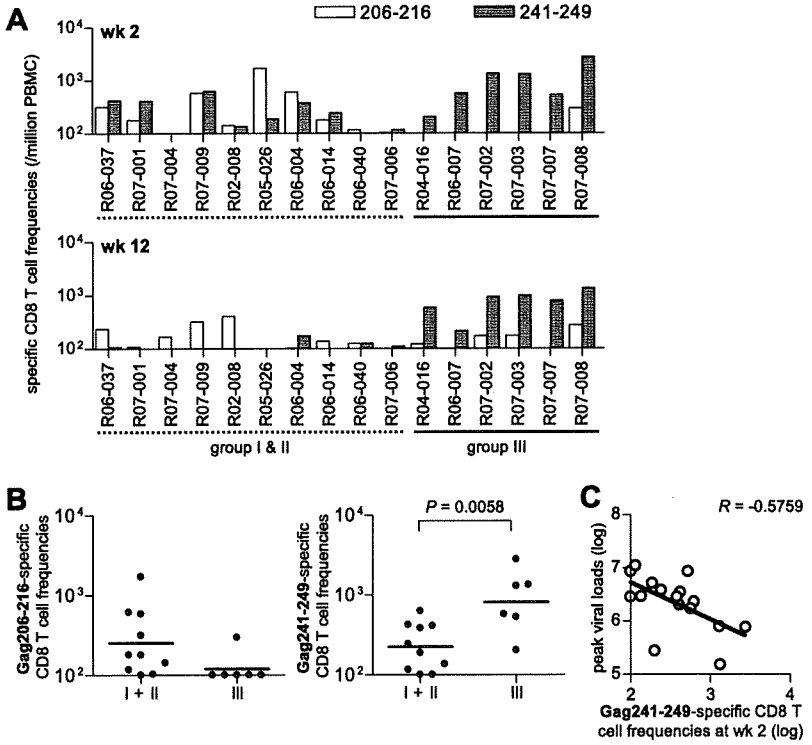

FIG. 3. Gag epitope-specific $CD8^+$ T-cell frequencies after a SIV challenge. (A) Frequencies of $CD8^+$ T cells (per million PBMCs) showing $Gag_{206\text{-}216}$-specific (open boxes) or $Gag_{241\text{-}249}$-specific (closed boxes) IFN-γ induction in naive controls and group III macaques at week 2 (upper panel) and week 12 (lower panel). (B) Comparison of the $Gag_{206\text{-}216}$-specific (left panel) or $Gag_{241\text{-}249}$-specific (right panel) $CD8^+$ T-cell frequencies in naive controls ($n = 10$) and group III animals ($n = 6$) at week 2. The bar indicates the geometric mean of each group. Frequencies of $Gag_{241\text{-}249}$-specific ($P = 0.0058$) but not $Gag_{206\text{-}216}$-specific ($P = 0.0922$) $CD8^+$ T cells in group III were significantly higher than in naive controls. The $Gag_{241\text{-}249}$-specific frequencies at week 12 in group III were significantly higher than those in naive controls ($P < 0.0001$). (C) Analysis of the correlation between $Gag_{241\text{-}249}$-specific $CD8^+$ T-cell frequencies (log) at week 2 and peak plasma viral loads (log). An inverse correlation is shown ($P = 0.0196$, $R = -0.5759$). Samples from macaques R02-007 and R06-019 in group I were unavailable for this analysis.

analysis revealed that this animal had $Gag_{241\text{-}249}$-specific granzyme B^+ IFN-γ^+ $CD8^+$ T cells. Indeed, group III animals had significantly higher frequencies of $Gag_{241\text{-}249}$-specific IFN-γ^+ $CD8^+$ T cells producing CD107a, granzyme B, or perforin ($P = 0.0076$; data not shown). These results indicate efficient induction of $Gag_{241\text{-}249}$-specific $CD8^+$ T cells with higher cytolytic activity in the acute phase in group III animals.

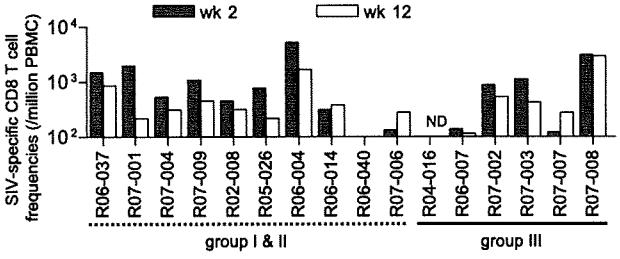

FIG. 4. SIV-specific $CD8^+$ T-cell frequencies after a SIV challenge. SIV-specific $CD8^+$ T-cell frequencies (per million PBMCs) in naive controls and group III macaques at week 2 (closed boxes) and week 12 (open boxes) are shown. ND, not determined.

DISCUSSION

In the present study, induction of $CD8^+$ T cells specific for a single $Gag_{241\text{-}249}$ epitope by prophylactic vaccination resulted in a significant reduction of plasma viral loads after a SIV challenge. Even if vaccines are designed to express multiple antigens, of the vaccine-induced $CD8^+$ T cells generated, at most one or only a few epitope-specific cells may recognize the incoming HIV because of viral diversity and host MHC polymorphisms (10). Our finding, however, implies that even a $CD8^+$ T-cell memory response to a single epitope which can recognize the incoming HIV could facilitate HIV control.

Group III macaques showed more effective $CD8^+$ T-cell responses than did naive controls after a SIV challenge. Our previous trial of a vaccine inducing Gag-specific T-cell responses resulted in SIV control in *90-120-Ia*-positive macaques with rapid selection of the GagL216S mutation escaping from $Gag_{206\text{-}216}$-specific $CD8^+$ T-cell recognition at week 5 (27). In contrast, the $Gag_{236\text{-}250}$ vaccination resulted in SIV control without *gag* mutation selection over 5 weeks in the present study, reflecting the fact that, rather than $Gag_{206\text{-}216}$-specific $CD8^+$ T-cell responses, dominantly induced $Gag_{241\text{-}249}$-specific $CD8^+$ T-cell responses played a central role in the reduc-

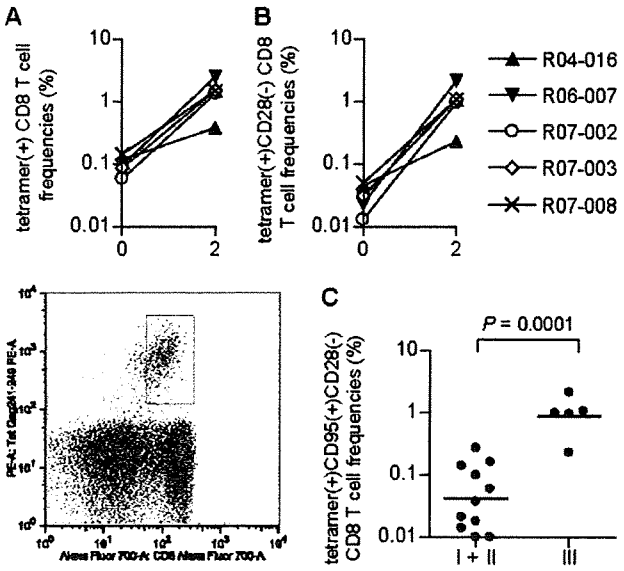

FIG. 5. Frequencies of $Gag_{241-249}$-specific $CD8^+$ T cells detected by $Gag_{241-249}$-Mamu-A*90120-5 tetramers after a SIV challenge. (A) Frequencies of $Gag_{241-249}$-Mamu-A*90120-5 $tetramer^+$ cells within $CD8^+$ T cells in group III animals before a challenge (week 0) or at week 2 after a challenge. A representative dot plot gated on $CD3^+$ lymphocytes for determining $tetramer^+$ $CD8^+$ T cells (x axis, CD8; y axis, tetramer) in macaque R07-008 is shown in the lower panel. (B) $Tetramer^+$ $CD28^-$ cell frequencies in $CD8^+$ T cells in group III animals at weeks 0 and 2. Data on $tetramer^+$ $CD95^+$ $CD28^-$ $CD8^+$ T-cell frequencies at week 0 are unavailable. (C) $Tetramer^+$ $CD95^+$ $CD28^-$ $CD8^+$ T-cell frequencies in naive controls (groups I and II) and group III animals at week 2. The bar indicates the geometric mean of each group. The frequencies in group III were significantly higher than those in naive controls ($P = 0.0001$ by unpaired t test). Samples from macaques R06-019 in group I and R07-007 in group III were unavailable for this analysis.

tion of viral loads in the acute phase. These results suggest that this vaccination approach altered the dominance pattern of $CD8^+$ T-cell responses and resulted in dominant induction of effective $Gag_{241-249}$-specific $CD8^+$ T-cell responses in the acute phase after a SIV challenge, facilitating a reduction in peak viral loads. Selection of vaccine epitopes for induction of $CD8^+$ T-cell responses might be important for viral control because the antiviral efficacy of $CD8^+$ T cells could be affected by MHC-I-restricted target epitopes (10, 19, 25, 35).

$Gag_{241-249}$-specific $CD8^+$ T-cell induction by prophylactic vaccination resulted in higher frequencies of these T-cell responses during the acute phase after the SIV challenge. The induction of $Gag_{241-249}$-specific effector memory $CD8^+$ T cells was especially marked. We did not examine polyfunctionality, but analyses of a cytolytic marker, CD107a, indicated higher frequencies of $Gag_{241-249}$-specific cytolytic $CD8^+$ T-cell responses, implying that these T cells originating from vaccine-induced memory may have higher cytolytic activity in the acute phase. These results suggest that group III animals with $Gag_{241-249}$-specific memory $CD8^+$ T cells showed induction of a high magnitude of $Gag_{241-249}$-specific $CD8^+$ T cells with effector function after a SIV challenge, resulting in reduction of viral loads in the acute phase.

In this study, some *90-120-Ia*-positive unvaccinated macaques showed lower viral loads. However, in our previous studies with Burmese rhesus macaques (reference 15 and unpublished data), all unvaccinated *90-120-Ia*-negative animals failed to contain a SIVmac239 challenge and animals, including vaccinees, that failed to control SIVmac239 replication developed AIDS in 1 to 4 years; even R-90-120 descendants possessing the MHC-I haplotype *90-120-Ib* but not *90-120-Ia* (both *90-120-Ia* and *90-120-Ib* are derived from breeder R-90-120) showed high viral loads. Additionally, *90-120-Ia*-positive animals failed to control the replication of SIVmac239 carrying CTL escape mutations (16). Thus, a SIVmac239 challenge of Burmese rhesus macaques mostly results in persistent viremia and progression to AIDS but some *90-120-Ia*-positive animals may show lower viral loads due to *90-120-Ia*-associated SIV-specific CTL responses. However, a previously reported *90-120-Ia*-positive unvaccinated macaque, R02-007, developed AIDS around 3 years after a SIVmac239 challenge. Furthermore, two of the *90-120-Ia*-positive vaccinees that controlled a SIVmac239 challenge but showed reappearance of viremia

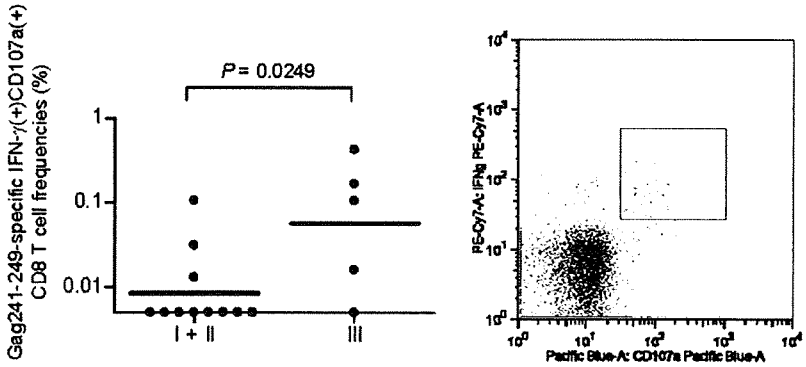

FIG. 6. $Gag_{241-249}$-specific cytolytic $CD8^+$ T-cell frequencies at week 2 after a challenge. PBMCs were cultured in the absence or the presence of the $Gag_{241-249}$ peptide for unstimulated controls or $Gag_{241-249}$-specific stimulation, and the frequencies of $CD8^+$ T cells exhibiting $Gag_{241-249}$-specific induction of both IFN-γ and CD107a in the total $CD8^+$ T cells were examined. The bar indicates the geometric mean of each group. The frequencies in group III were significantly higher than those in naive controls ($P = 0.0249$ by unpaired t test). The right panel is a representative dot plot showing the CD107a (x axis) and IFN-γ (y axis) responses in $CD8^+$ T cells in macaque R07-008 after $Gag_{241-249}$-specific stimulation. Samples from macaques R06-019 in group I and R07-007 in group III were unavailable for this analysis.

around 1 year later developed AIDS (15). Thus, it is inferred that the majority of *90-120-Ia*-positive unvaccinated macaques develop AIDS after a SIVmac239 challenge. Several MHC-I alleles are known to be associated with lower viral loads in HIV and SIV infections, and potent CTLs directed against these MHC-I-restricted epitopes have been implicated in the suppression of viral replication (7, 8, 9, 10, 13, 18, 22, 31, 33, 48). The $Gag_{241-249}$-specific CTL may also be naturally potent (10, 16), but the impact of memory induction of even these potent CTLs on viral control has not yet been determined. Thus, this is the first study documenting the benefit of single-epitope-specific memory $CD8^+$ T-cell induction by prophylactic vaccination for HIV/SIV control. Further analysis with a vaccine expressing a single helper epitope, as well as a CTL epitope, would contribute to evaluation of the impact of HIV/SIV-specific $CD4^+$ T-cell memory induction on HIV/SIV replication.

Because $CCR5^+$ memory $CD4^+$ T cells, especially HIV-specific $CD4^+$ T cells, are themselves targets of this virus, whether virus-specific $CD4^+$ T-cell induction by prophylactic vaccination can result in effective virus-specific $CD4^+$ T-cell responses postinfection and contribute to HIV control remains unclear. On the other hand, it has been unknown whether HIV-specific memory $CD8^+$ T cells induced by vaccination without HIV-specific $CD4^+$ T-cell help can elicit effective responses after virus exposure. In the present study, the $pGag_{236-250}$-EGFP/F(−)SeV-$Gag_{236-250}$-EGFP vaccination elicited $Gag_{241-249}$-specific $CD8^+$ T-cell responses without SIV-specific $CD4^+$ T-cell help but possibly with EGFP-specific or SeV-specific $CD4^+$ T-cell help; i.e., SeV-EGFP-specific $CD4^+$ T cells would confer cognate help for $Gag_{241-249}$-specific $CD8^+$ T-cell induction. The $Gag_{241-249}$-specific memory $CD8^+$ T cells induced by prophylactic vaccination without SIV-specific $CD4^+$ T-cell help but with non-SIV-specific $CD4^+$ T-cell responses responded efficiently to a SIV challenge, showing dominant $Gag_{241-249}$-specific $CD8^+$ T-cell responses resulting in SIV control; infection-induced SIV-specific $CD4^+$ T-cell responses may be involved in $Gag_{241-249}$-specific $CD8^+$ T-cell induction postinfection. Therefore, this study documents that prophylactic vaccination eliciting virus-specific $CD8^+$ T-cell memory even without virus-specific $CD4^+$ T-cell responses (but with cognate non-virus-specific $CD4^+$ T-cell responses) can facilitate SIV control after a challenge.

Taken together, the present study demonstrates that induction of single-epitope-specific $CD8^+$ T-cell memory without virus-specific $CD4^+$ T-cell help by prophylactic vaccination can result in dominant potent $CD8^+$ T-cell responses and control of SIV replication after a challenge. These results imply possible HIV control by prophylactic vaccination eliciting virus-specific $CD8^+$ T-cell memory with non-virus-specific $CD4^+$ T-cell help and provide valuable insights into AIDS vaccine development.

ACKNOWLEDGMENTS

This work was supported by grants from the Ministry of Education, Culture, Sports, Science, and Technology and grants from the Ministry of Health, Labor, and Welfare in Japan. The animal experiments were conducted through the Cooperative Research Program in the Tsukuba Primate Research Center, National Institute of Biomedical Innovation, with the help of the Corporation for Production and Research of Laboratory Primates.

We thank H. Akari, Y. Yasutomi, F. Ono, A. Hiyaoka, K. Komatsuzaki, K. Oto, K. Ishikawa, and T. Nakasone for their assistance in animal experiments; DNAVEC Corp. for providing SeV vectors; M. Roederer for providing the PESTLE and SPICE software; and Y. Tsunetsugu-Yokota, H. Igarashi, A. Kimura, T. Naruse, M. Miyazawa, K. Mori, N. Yamamoto, A. Nomoto, and Y. Nagai for their help.

REFERENCES

1. **Anonymous.** 2007. Cold shower for AIDS vaccines. Nat. Med. **13**:1389–1390.
2. **Argüello, J. R., A. M. Little, A. L. Pay, D. Gallardo, I. Rojas, S. G. Marsh, J. M. Goldman, and J. A. Madrigal.** 1998. Mutation detection and typing of polymorphic loci through double-strand conformation analysis. Nat. Genet. **18**:192–194.
3. **Borrow, P., H. Lewicki, B. H. Hahn, G. M. Shaw, and M. B. Oldstone.** 1994. Virus-specific $CD8^+$ cytotoxic T-lymphocyte activity associated with control of viremia in primary human immunodeficiency virus type 1 infection. J. Virol. **68**:6103–6110.
4. **Brander, C., and B. D. Walker.** 1999. T lymphocyte responses in HIV-1 infection: implication for vaccine development. Curr. Opin. Immunol. **11**: 451–459.
5. **Douek, D. C., J. M. Brenchley, M. R. Betts, D. R. Ambrozak, B. J. Hill, Y. Okamoto, J. P. Casazza, J. Kuruppu, K. Kunstman, S. Wolinsky, Z. Grossman, M. Dybul, A. Oxenius, D. A. Price, M. Connors, and R. A. Koup.** 2002. HIV preferentially infects HIV-specific $CD4^+$ T cells. Nature **417**:95–98.
6. **Feinberg, M. B., and J. P. Moore.** 2002. AIDS vaccine models: challenging challenge viruses. Nat. Med. **8**:207–210.
7. **Friedrich, T. C., E. J. Dodds, L. J. Yant, L. Vojnov, R. Rudersdorf, C. Cullen, D. T. Evans, R. C. Desrosiers, B. R. Mothe, J. Sidney, A. Sette, K. Kunstman, S. Wolinsky, M. Piatak, J. Lifson, A. L. Hughes, N. Wilson, D. H. O'Connor, and D. I. Watkins.** 2004. Reversion of CTL escape-variant immunodeficiency viruses in vivo. Nat. Med. **10**:275–281.
8. **Goulder, P. J., M. Bunce, P. Krausa, K. McIntyre, S. Crowley, B. Morgan, A. Edwards, P. Giangrande, R. E. Phillips, and A. J. McMichael.** 1996. Novel, cross-restricted, conserved, and immunodominant cytotoxic T lymphocyte epitopes in slow progressors in HIV type 1 infection. AIDS Res. Hum. Retrovir. **12**:1691–1698.
9. **Goulder, P. J., and D. I. Watkins.** 2004. HIV and SIV CTL escape: implications for vaccine design. Nat. Rev. Immunol. **4**:630–640.
10. **Goulder, P. J. R., and D. I. Watkins.** 2008. Impact of MHC class I diversity on immune control of immunodeficiency virus replication. Nat. Rev. Immunol. **8**:619–630.
11. **Janssen, E. M., E. E. Lemmens, T. Wolfe, U. Christen, M. G. von Herrath, and S. P. Schoenberger.** 2003. $CD4^+$ T cells are required for secondary expansion and memory in $CD8^+$ T lymphocytes. Nature **421**:852–856.
12. **Jin, X., D. E. Bauer, S. E. Tuttleton, S. Lewin, A. Gettie, J. Blanchard, C. E. Irwin, J. T. Safrit, J. Mittler, L. Weinberger, L. G. Kostrikis, L. Zhang, A. S. Perelson, and D. D. Ho.** 1999. Dramatic rise in plasma viremia after $CD8^+$ T cell depletion in simian immunodeficiency virus-infected macaques. J. Exp. Med. **189**:991–998.
13. **Kaslow, R. A., M. Carrington, R. Apple, L. Park, A. Muñoz, A. J. Saah, J. J. Goedert, C. Winkler, S. J. O'Brien, C. Rinaldo, R. Detels, W. Blattner, J. Phair, H. Erlich, and D. L. Mann.** 1996. Influence of combinations of human major histocompatibility complex genes on the course of HIV-1 infection. Nat. Med. **2**:405–411.
14. **Kawada, M., H. Igarashi, A. Takeda, T. Tsukamoto, H. Yamamoto, S. Dohki, M. Takiguchi, and T. Matano.** 2006. Involvement of multiple epitope-specific cytotoxic T-lymphocyte responses in vaccine-based control of simian immunodeficiency virus replication in rhesus macaques. J. Virol. **80**:1949–1958.
15. **Kawada, M., T. Tsukamoto, H. Yamamoto, A. Takeda, H. Igarashi, D. I. Watkins, and T. Matano.** 2007. Long-term control of simian immunodeficiency virus replication with central memory $CD4^+$ T-cell preservation after nonsterile protection by a cytotoxic T-lymphocyte-based vaccine. J. Virol. **81**:5202–5211.
16. **Kawada, M., T. Tsukamoto, H. Yamamoto, N. Iwamoto, K. Kurihara, A. Takeda, C. Moriya, H. Takeuchi, H. Akari, and T. Matano.** 2008. Gag-specific cytotoxic T lymphocyte-based control of primary simian immunodeficiency virus replication in a vaccine trial. J. Virol. **82**:10199–10206.
17. **Kestler, H. W., III, D. J. Ringler, K. Mori, D. L. Panicali, P. K. Sehgal, M. D. Daniel, and R. C. Desrosiers.** 1991. Importance of the nef gene for maintenance of high virus loads and for development of AIDS. Cell **65**:651–662.
18. **Kiepiela, P., A. J. Leslie, I. Honeyborne, D. Ramduth, C. Thobakgale, S. Chetty, P. Rathnavalu, C. Moore, K. J. Pfafferott, L. Hilton, P. Zimbwa, S. Moore, T. Allen, C. Brander, M. M. Addo, M. Altfeld, I. James, S. Mallal, M. Bunce, L. D. Barber, J. Szinger, C. Day, P. Klenerman, J. Mullins, B. Korber, H. M. Coovadia, B. D. Walker, and P. J. Goulder.** 2004. Dominant influence of HLA-B in mediating the potential co-evolution of HIV and HLA. Nature **432**:769–775.
19. **Kiepiela, P., K. Ngumbela, C. Thobakgale, D. Ramduth, I. Honeyborne, E. Moodley, S. Reddy, C. de Pierres, Z. Mncube, N. Mkhwanazi, K. Bishop, M. van der Stok, K. Nair, N. Khan, H. Crawford, R. Payne, A. Leslie, J. Prado,**

A. Prendergast, J. Frater, N. McCarthy, C. Brander, G. H. Learn, D. Nickle, C. Rousseau, H. Coovadia, J. I. Mullins, D. Heckerman, B. D. Walker, and P. Goulder. 2007. CD8+ T-cell responses to different HIV proteins have discordant associations with viral load. Nat. Med. 13:46–53.
20. Koup, R. A., J. T. Safrit, Y. Cao, C. A. Andrews, G. McLeod, W. Borkowsky, C. Farthing, and D. D. Ho. 1994. Temporal association of cellular immune responses with the initial control of viremia in primary human immunodeficiency virus type 1 syndrome. J. Virol. 68:4650–4655.
21. Lamoreaux, L., M. Roederer, and R. Koup. 2006. Intracellular cytokine optimization and standard operating procedure. Nat. Protoc. 1:1507–1516.
22. Leslie, A. J., K. J. Pfafferott, P. Chetty, R. Draenert, M. M. Addo, M. Feeney, Y. Tang, E. C. Holmes, T. Allen, J. G. Prado, M. Altfeld, C. Brander, C. Dixon, D. Ramduth, P. Jeena, S. A. Thomas, A. St. John, T. A. Roach, B. Kupfer, G. Luzzi, A. Edwards, G. Taylor, H. Lyall, G. Tudor-Williams, V. Novelli, J. Martinez-Picado, P. Kiepiela, B. D. Walker, and P. J. Goulder. 2004. HIV evolution: CTL escape mutation and reversion after transmission. Nat. Med. 10:282–289.
23. Letvin, N. L., J. R. Mascola, Y. Sun, D. A. Gorgone, A. P. Buzby, L. Xu, Z. Y. Yang, B. Chakrabarti, S. S. Rao, J. E. Schmitz, D. C. Montefiori, B. R. Barker, F. L. Bookstein, and G. J. Nabel. 2006. Preserved CD4+ central memory T cells and survival in vaccinated SIV-challenged monkeys. Science 312:1530–1533.
24. Li, H. O., Y. F. Zhu, M. Asakawa, H. Kuma, T. Hirata, Y. Ueda, Y. S. Lee, M. Fukumura, A. Iida, A. Kato, Y. Nagai, and M. Hasegawa. 2000. A cytoplasmic RNA vector derived from nontransmissible Sendai virus with efficient gene transfer and expression. J. Virol. 74:6564–6569.
25. Loffredo, J. T., A. T. Bean, D. R. Beal, E. J. León, G. E. May, S. M. Piaskowski, J. R. Furlott, J. Reed, S. K. Musani, E. G. Rakasz, T. C. Friedrich, N. A. Wilson, D. B. Allison, and D. I. Watkins. 2008. Patterns of CD8+ immunodominance may influence the ability of Mamu-B*08-positive macaques to naturally control simian immunodeficiency virus SIVmac239 replication. J. Virol. 82:1723–1738.
26. Matano, T., M. Kano, H. Nakamura, A. Takeda, and Y. Nagai. 2001. Rapid appearance of secondary immune responses and protection from acute CD4 depletion after a highly pathogenic immunodeficiency virus challenge in macaques vaccinated with a DNA-prime/Sendai viral vector-boost regimen. J. Virol. 75:11891–11896.
27. Matano, T., M. Kobayashi, H. Igarashi, A. Takeda, H. Nakamura, M. Kano, C. Sugimoto, K. Mori, A. Iida, T. Hirata, M. Hasegawa, T. Yuasa, M. Miyazawa, Y. Takahashi, M. Yasunami, A. Kimura, D. H. O'Connor, D. I. Watkins, and Y. Nagai. 2004. Cytotoxic T lymphocyte-based control of simian immunodeficiency virus replication in a preclinical AIDS vaccine trial. J. Exp. Med. 199:1709–1718.
28. Matano, T., R. Shibata, C. Siemon, M. Connors, H. C. Lane, and M. A. Martin. 1998. Administration of an anti-CD8 monoclonal antibody interferes with the clearance of chimeric simian/human immunodeficiency virus during primary infections of rhesus macaques. J. Virol. 72:164–169.
29. Mattapallil, J. J., N. L. Letvin, and M. Roederer. 2004. T-cell dynamics during acute SIV infection. AIDS 18:13–23.
30. McMichael, A. J., and T. Hanke. 2003. HIV vaccines 1983-2003. Nat. Med. 9:874–880.
31. Migueles, S. A., M. S. Sabbaghian, W. L. Shupert, M. P. Bettinotti, F. M. Marincola, L. Martino, C. W. Hallahan, S. M. Selig, D. Schwartz, J. Sullivan, and M. Connors. 2000. HLA B*5701 is highly associated with restriction of virus replication in a subgroup of HIV-infected long term nonprogressors. Proc. Natl. Acad. Sci. USA 97:2709–2714.
32. National Institute of Infectious Diseases. 2007. Guides for animal experiments performed at National Institute of Infectious Diseases. National Institute of Infectious Diseases, Tokyo, Japan. (In Japanese.)
33. O'Connor, D. H., B. R. Mothe, J. T. Weinfurter, S. Fuenger, W. M. Rehrauer, P. Jing, R. R. Rudersdorf, M. E. Liebl, K. Krebs, J. Vasquez, E. Dodds, J. Loffredo, S. Martin, A. B. McDermott, T. M. Allen, C. Wang, G. G. Doxiadis, D. C. Montefiori, A. Hughes, D. R. Burton, D. B. Allison, S. M. Wolinsky, R. Bontrop, L. J. Picker, and D. I. Watkins. 2003. Major histocompatibility complex class I alleles associated with slow simian immunodeficiency virus disease progression bind epitopes recognized by dominant acute-phase cytotoxic-T-lymphocyte responses. J. Virol. 77:9029–9040.
34. Pitcher, C. J., S. I. Hagen, J. M. Walker, R. Lum, B. L. Mitchell, V. C. Maino, M. K. Axthelm, and L. J. Picker. 2002. Development and homeostasis of T cell memory in rhesus macaques. J. Immunol. 168:29–43.
35. Reynolds, M. R., A. M. Weiler, K. L. Weisgrau, S. M. Piaskowski, J. R. Furlott, J. T. Weinfurter, M. Kaizu, T. Soma, E. J. León, C. MacNair, D. P. Leaman, M. B. Zwick, E. Gostick, S. K. Musani, D. A. Price, T. C. Friedrich, E. G. Rakasz, N. A. Wilson, A. B. McDermott, R. Boyle, D. B. Allison, D. R. Burton, W. C. Koff, and D. I. Watkins. 2008. Macaques vaccinated with live-attenuated SIV control replication of heterologous virus. J. Exp. Med. 205:2537–2550.
36. Rosenberg, E. S., J. M. Billingsley, A. M. Caliendo, S. L. Boswell, P. E. Sax, S. A. Kalams, and B. D. Walker. 1997. Vigorous HIV-1-specific CD4+ T cell responses associated with control of viremia. Science 278:1447–1450.
37. Schmitz, J. E., M. J. Kuroda, S. Santra, V. G. Sasseville, M. A. Simon, M. A. Lifton, P. Racz, K. Tenner-Racz, M. Dalesandro, B. J. Scallon, J. Ghrayeb, M. A. Forman, D. C. Montefiori, E. P. Rieber, N. L. Letvin, and K. A. Reimann. 1999. Control of viremia in simian immunodeficiency virus infection by CD8+ lymphocytes. Science 283:857–860.
38. Seder, R. A., P. A. Darrah, and M. Roederer. 2008. T-cell quality in memory and protection: implications for vaccine design. Nat. Rev. Immunol. 8:247–258.
39. Shaffer, J. P. 1986. Modified sequentially rejective multiple test procedures. J. Am. Stat. Assoc. 81:826–831.
40. Shedlock, D. J., and H. Shen. 2003. Requirement for CD4 T cell help in generating functional CD8 T cell memory. Science 300:337–339.
41. Shibata, R., F. Maldarelli, C. Siemon, T. Matano, M. Parta, G. Miller, T. Fredrickson, and M. A. Martin. 1997. Infection and pathogenicity of chimeric simian-human immunodeficiency viruses in macaques: determinants of high virus loads and CD4 cell killing. J. Infect. Dis. 176:362–373.
42. Staprans, S. I., A. P. Barry, G. Silvestri, J. T. Safrit, N. Kozyr, B. Sumpter, H. Nguyen, H. McClure, D. Montefiori, J. I. Cohen, and M. B. Feinberg. 2004. Enhanced SIV replication and accelerated progression to AIDS in macaques primed to mount a CD4 T cell response to the SIV envelope protein. Proc. Natl. Acad. Sci. USA 101:13026–13031.
43. Sun, J. C., and M. J. Bevan. 2003. Defective CD8 T cell memory following acute infection without CD4 T cell help. Science 300:339–342.
44. Tanaka-Takahashi, Y., M. Yasunami, T. Naruse, K. Hinohara, T. Matano, K. Mori, M. Miysazawa, M. Honda, Y. Yasutomi, Y. Nagai, and A. Kimura. 2007. Reference strand-mediated conformation analysis (RSCA)-based typing of multiple alleles in the rhesus macaque MHC class I Mamu-A and Mamu-B loci. Electrophoresis 28:918–924.
45. Tsukamoto, T., S. Dohki, T. Ueno, M. Kawada, A. Takeda, M. Yasunami, T. Naruse, A. Kimura, M. Takiguchi, and T. Matano. 2008. Determination of a major histocompatibility complex class I restricting simian immunodeficiency virus Gag241-249 epitope. AIDS 22:993–994.
46. Vaccari, M., J. Mattapallil, K. Song, W. P. Tsai, A. Hryniewicz, D. Venzon, M. Zanetti, K. A. Reimann, M. Roederer, and G. Franchini. 2008. Reduced protection from simian immunodeficiency virus SIVmac251 infection afforded by memory CD8+ T cells induced by vaccination during CD4+ T-cell deficiency. J. Virol. 82:9629–9638.
47. Wilson, N. A., J. Reed, G. S. Napoe, S. Piaskowski, A. Szymanski, J. Furlott, E. J. Gonzalez, L. J. Yant, N. J. Maness, G. E. May, T. Soma, M. R. Reynolds, E. Rakasz, R. Rudersdorf, A. B. McDermott, D. H. O'Connor, T. C. Friedrich, D. B. Allison, A. Patki, L. J. Picker, D. R. Burton, J. Lin, L. Huang, D. Patel, G. Heindecker, J. Fan, M. Citron, M. Horton, F. Wang, X. Liang, J. W. Shiver, D. R. Casimiro, and D. I. Watkins. 2006. Vaccine-induced cellular immune responses reduce plasma viral concentrations after repeated low-dose challenge with pathogenic simian immunodeficiency virus SIVmac239. J. Virol. 80:5875–5885.
48. Yant, L. J., T. C. Friedrich, R. C. Johnson, G. E. May, N. J. Maness, A. M. Enz, J. D. Lifson, D. H. O'Connor, M. Carrington, and D. I. Watkins. 2006. The high-frequency major histocompatibility complex class I allele Mamu-B*17 is associated with control of simian immunodeficiency virus SIVmac239 replication. J. Virol. 80:5074–5077.

Journal of Human Genetics (2009) 54, 224–229

www.nature.com/jhg

ORIGINAL ARTICLE

Complex divergence at a microsatellite marker *C1_2_5* in the lineage of *HLA-Cw/-B* haplotype

Daisuke Shichi[1], Masao Ota[2], Yoshihiko Katsuyama[3], Hidetoshi Inoko[4], Taeko K Naruse[1] and Akinori Kimura[1,5]

The human leukocyte antigen (HLA) complex locus has shaped a framework for evolutionary processes because of the dense clustering and strong linkage disequilibrium (LD) of polymorphic genes. Although the landscape of LD among conventional single-nucleotide polymorphisms (SNPs) has been described, the data on the lineage of major histocompatibility complex (MHC) haplotype are limited to pairwise comparisons of several haplotypes in Caucasoid populations. Multi-allelic markers, including microsatellite markers, may provide us with a larger power to analyze the MHC haplotype lineage because the mutation rate of microsatellite exceeds that of SNPs by several orders of magnitude. In this study, we investigated the complex structure of repeat motifs in a microsatellite to figure out the structural lineage of *HLA-Cw/-B* segments in Japanese. It was found that the genetic differences of *HLA-Cw/-B* haplotype lineage were reflected by repeat motif patterns at *C1_2_5* locus, suggesting that unique mutational dynamics of microsatellites may be a useful marker to chase the haplotype lineage.
Journal of Human Genetics (2009) **54**, 224–229; doi:10.1038/jhg.2009.15; published online 27 February 2009

Keywords: C1_2_5; HLA; microsatellite; repeat motif

INTRODUCTION

The human major histocompatibility complex (MHC), the human leukocyte antigen locus (HLA) on chromosome 6p21.3, spans about 4 Mb and contains many polymorphic genes relevant to the adaptive immune system.[1] Among them, genes for classical HLA molecules play pivotal roles in the immunological recognition of self versus non-self through presentation of antigenic peptides from either intracellular or extracellular origin.[2] Most of the extensive polymorphisms in the *HLA* genes were found at the peptide-binding groove of HLA molecules, thereby defining the bound peptides.[3] The HLA alleles at a given locus differ from each other by 1–30 amino acids at the protein level[4] and have been designated by the four-digit number or more according to the patterns of single-nucleotide polymorphisms (SNPs) and insertion–deletion polymorphisms within the coding sequence. The difference in allele distribution among different ethnic groups may be shaped by selective and demographic history.[5] It is well known that there is a strong linkage disequilibrium (LD) among alleles of genes in *HLA* locus, and combination of these alleles in LD form specific haplotypes.[6] Owing to the functional significance of classical *HLA* genes, the MHC haplotypes have been defined by using classical *HLA* alleles as highly polymorphic markers, and the *HLA* haplotypes served as a model system for high-resolution mapping of disease susceptibility genes,[7] evolution[8] and population structure.[9]

Detailed information on allelic diversity, recombination hotspot and profiles of LD within the MHC region are available,[6] but data on the lineage of the MHC haplotype and its evolution are not complete. The MHC Haplotype Sequencing Project was designed to elucidate the complete MHC genetic maps of several common Caucasian MHC haplotypes,[10] but little information is available for MHC haplotypes from different ethnic groups other than that from the Caucasians. Using selected genomic variation, including SNPs, individual MHC haplotypes can be characterized. This strategy has been used extensively to resolve the structure of the *HLA* allelic composition of SNPs and to determine new *HLA* alleles.[11] However, conventional SNP-based tagging could not adequately provide a resolution to capture the characteristics of variations of the MHC region at the worldwide population level. In other words, genetic markers other than SNPs, including copy number variations (CNVs) and microsatellites, might provide additional information in tracing the differentiation of the MHC haplotype.

Microsatellites, in general, undergo rapid change because of the insertion or deletion of one or multiple repeat units, primarily through replication slippage.[12] Moreover, the mutation rate of microsatellites (10^{-5}–10^{-3} per generation) exceeds that of SNPs and CNVs by several orders of magnitude. The difference in the mutational dynamics suggested that the microsatellites may be useful in tracing recent divergence in the structure of MHC haplotypes. More than

[1]Department of Molecular Pathogenesis, Medical Research Institute, Tokyo Medical and Dental University, Tokyo, Japan; [2]Department of Legal Medicine, Shinshu University School of Medicine, Matsumoto, Japan; [3]Department of Pharmacy, Shinshu University Hospital, Matsumoto, Japan; [4]Department of Molecular Life Science, Tokai University School of Medicine, Isehara, Japan and [5]Laboratory of Genome Diversity, School of Biomedical Science, Tokyo Medical and Dental University, Tokyo, Japan
Correspondence: Professor A Kimura, Department of Molecular Pathogenesis, Medical Research Institute, Tokyo Medical and Dental University, 1-5-45 Yushima, Bunkyo-ku, Tokyo 113-8510, Japan.
E-mail: akitis@mri.tmd.ac.jp
Received 17 November 2008; revised 3 February 2009; accepted 4 February 2009; published online 27 February 2009

1000 polymorphic microsatellite markers have been described within the *HLA* region.[13–16] The microsatellite markers showed considerable polymorphism and strong LD with particular alleles of classical *HLA* loci composing of well-defined extended *HLA* haplotypes.[17] The *HLA* haplotypes can be separated into several blocks, including a haplotype block containing the *HLA-Cw* and *-B* genes, just centromeric to the MHC class I region, which is known to be one of the highest polymorphic loci in the human genome.[18] In this study, we analyzed the microsatellite diversity surrounding the *HLA-Cw/-B* loci to investigate the haplotype lineages in a Japanese population.

MATERIALS AND METHODS

Study population and genotyping methods

The study population consisted of 261 Japanese individuals selected at random. All subjects gave informed consent and the study was approved by the Research Ethics Committee of Medical Research Institute, Tokyo Medical and Dental University and Tokai University School of Medicine. Complete genotyping was achieved for classical *HLA* genes and nine microsatellite markers from all individuals were enrolled in this study. Deviation from the Hardy–Weinberg equilibrium was tested for each *HLA* locus and each microsatellite marker. None of the selected markers showed significant ($P<0.05$) deviation from the Hardy–Weinberg equilibrium. High-resolution *HLA* genotyping (at four-digit allele resolution) was carried out with a sequence-based typing method at the class I genes (*HLA-A*, *-B* and *-Cw*) as recommended by the 13th International Histocompatibility Workshop protocols (http://www.ihwg.org/) and/or manufacturer's instructions (Forensic Analytical, Hayward, CA, USA). When an ambiguity in the genotype assignment was observed in the sequence trace data, genotype was predicted from the allele frequency and LD information in the Japanese.[19] DNA regions spanning the microsatellite polymorphisms were amplified by PCR using primer pairs under the conditions listed in Table 1, and the sequenced reference B-cell line samples, COX and PGX, were used as standard for sizing assignment of microsatellite.[20] In addition, to show the motif variation at *C1_2_5* locus, we sequenced the PCR products obtained from each subject on both strands. The number of repeat units was determined by the direct sequencing along with the fragment length analysis. A part (about 38%) of the subjects was also investigated for the *C1_2_5* allele by cloning the PCR products using the TA cloning kit (Invitrogen, Carlsbad, CA, USA). Data from the cloning of *C1_2_5* were completely consistent with the genotyping data obtained from the direct sequencing method.

Phylogenetic analysis

Sequence data on the *HLA-Cw* alleles (exon 4) were obtained from the IMGT/HLA sequence database (http://www.ebi.ac.uk/imgt/hla/index.html). Sequence alignments of the alleles were created by using GENETYX version 8.1.2 (GENETYX CORPORATION, Tokyo, Japan). Phylogenetic analyses were performed using the unweighted pair group method using arithmetic average (UPGMA) by the MEGA software Version 4.0 (http://www.megasoftware.net/).

Statistical analysis

Deviation from the Hardy–Weinberg equilibrium was tested for all marker loci by using the PyPop v.0.6.0 software package (http://www.pypop.org/).[21] The expectation–maximization algorithm implemented in the 'haplo_stat' package for R statistics software (http://www.r-project.org/)[22] was used to construct haplotypes and estimate their frequencies. The strength of pairwise LD between the alleles of classical *HLA* genes and/or microsatellite markers was quantified by two LD coefficients, D' and r^2, through the add-on R software package 'genetics'.[23] We also evaluated the associations between the *HLA-B* and *HLA-Cw* alleles by sensitivity and specificity; sensitivity was defined as the probability of observing the *HLA-B* allele when a particular *HLA-Cw* allele was observed, whereas specificity was the probability of not observing the *HLA-B* allele in the absence of the particular *HLA-Cw* allele. The long-range association was investigated by the extended haplotype homozygosity (EHH) statistic that was calculated according to the formula developed by Sabeti *et al.*[24] Overall LDs between two loci were estimated by using two statistics, Hedrick's multi-allelic D'[25] and Cramer's V.[26] When there are only two alleles per locus, Cramer's V is equivalent to the correlation coefficient between the two loci. Statistical significance of the LD between pairs of loci was tested using a permutation test with 1000 permutations for each locus pair.

RESULTS

Association between *HLA-B* and *-Cw* gene loci

Significant associations between the alleles of *HLA-Cw* and *HLA-B* genes were found among 261 Japanese individuals as expected from the physical proximity of *HLA-Cw* and *-B* (85 kb). Of the 75 different

Table 1 Primer sets for microsatellite genotyping around the *HLA-B/-Cw* loci

Marker name	*Position*[a]	*Repeat unit*	*PCR product size (bp)*	*Primer sequence (5′–3′)*	*Dye*	*PCR condition*[b]
C2_4_4	31697425–31697663	(GAAA)	181–281	GGCTTGACTTGAAACTCAGAGACC	Hex	i
				TTATCTACTTATAGTCTATCACGG	—	
C1_3_1	31884120–31884408	(TTG)	279–345	CAGTGACAAGCACCTGGCAC	Tet	i
				GCCAGATGTGGTGGCATGC	—	
C1_2_5	31367081–31367280	(CA)	178–220	CAGTAGTAAGCCAGAAGCTATTAC	6-Fam	i
				AAGTCAAGCATATCTGCCATTTGG	—	
C1_4_1	31439129–31439353	(AAAC)	171–271	CGAGAGAACAACTGGCAGGACTG	6-Fam	i
				GACAGTCCTCATTAGCGCTGAGG	—	
MIB	31457335–31457670	(CA)	326–356	CTACCATGACCCCCTTCCCC	Hex	i
				CCACAGTCTCTATCAGTCCA	—	
STR_MICA	31488069–31488251	(GCT)	179–194	CCTTTTTTTCAGGGAAAGTGC	6-Fam	i
				CCTTACCATCTCCAGAAACTGC	—	
C1_2_A	31579685–31579926	(CA)	234–264	AATAGCCATGAGAAGCTATGTGGGGGAG	6-Fam	ii
				CTACCTCCTTGCCAAACTTGCTGTTTGTG	—	
TNFa	31643387–31643503	(AC)	61–161	CCTCTCTCCCCTGCAACACACA	6-Fam	i
				GCCTCTAGATTTCATCCAGCCACA	—	
TNFd	31664102–31664231	(TC)	131–137	AGATCCTTCCCTGTGAGTTCTGCT	Hex	i
				CATAGTGGGACTCTGTCTCCAAAG	—	

[a]The chromosome 6 genomic sequences was used as a reference.
[b]The PCR was carried out in an ABI9700 thermal cycler under the following conditions: (i) 12 min at 95 °C followed by 35 cycles of 95 °C for 30 s, 55 °C for 45 s, 72 °C for 1 min and final extension for 10 min at 72 °C; (ii) 2 min at 94 °C followed by 30 cycles of 94 °C for 1 min, 55 °C for 1 min, 72 °C for 2 min, with an additional 5 min final extension at 72 °C.

Table 2 Association performance of *HLA-Cw/-B* haplotypes in a Japanese population

HLA-B/-Cw haplotype	*Haplotype frequency*	*D'*	*Hill's r^2*	*Sensitivity[a] (%)*	*Specificity[b] (%)*
*Cw*1202-B*5201*	0.144	0.98	0.93	97.4	98.9
*Cw*0102-B*5401*	0.092	0.94	0.32	94.1	84.9
*Cw*0303-B*1501*	0.036	0.40	0.12	45.2	92.3
*Cw*0304-B*4002*	0.054	0.77	0.34	77.8	93.4
*Cw*0102-B*4601*	0.057	0.91	0.19	90.9	81.8
*Cw*0702-B*0702*	0.061	0.96	0.43	97.0	93.0
*Cw*0303-B*3501*	0.042	0.66	0.24	68.8	93.1
*Cw*0304-B*4001*	0.034	0.53	0.14	58.1	91.4
*Cw*1403-B*4403*	0.057	1.00	0.93	96.8	99.8
*Cw*1402-B*5101*	0.048	0.06	0.76	80.6	99.8

[a]Sensitivity: the probability of observing the particular *HLA-Cw* allele given the presence of the particular *HLA-B* allele.
[b]Specificity: the probability of not observing the particular *HLA-Cw* allele given the absence of the particular *HLA-B* allele.

HLA-B and *-Cw* allele combinations observed, 10 were relatively common with haplotype frequency above 3%, by which 63% of the Japanese panels could be explained (Table 2). Two combinations, *Cw*1202-B*5201* and *Cw*1403-B*4403*, showed high correlations (over 0.90) for sensitivity, specificity, *D'* and r^2. In contrast, *HLA-Cw/-B* haplotypes containing *Cw*0102*, *Cw*0303* and *Cw*0304* showed less association, although these haplotypes could account for a considerable part in the Japanese population, because these *HLA-Cw* alleles composed of several haplotypes with different *HLA-B* alleles.

Long-range haplotype around the *HLA-B* and *-Cw* genes

To analyze a long-range structure of the region, EHH analysis was performed, which enabled us to estimate the length of LD from the alleles of a landmark locus. As illustrated in Figure 1, each EHH profile within the 300 kb from the landmark tended to decline the LD with increasing distance from the landmark as expected. However, the pattern of EHH varied substantially, depending on the allele at the landmark locus and on the two-locus haplotype. The haplotypes landmarked by the alleles of *HLA-Cw* and *-B* genes extended longer to telomeric side (MHC class I region) and centromeric side (MHC class II region), respectively (Figures 1a–d). Nevertheless, *HLA-Cw/-B* haplotypic combinations (for example, *Cw*1202* and *B*5201*, *Cw*1403* and *B*4403*) formed by almost one-to-one correspondence showed the long-range LD. In clear contrast, others (for example, *Cw*0102*, *Cw *0303* and *Cw *0304*) with highly diverged combinations rapidly diminished the EHH score even within approximately 100 kb around the landmark locus (Figure 1b). As a rapid EHH decay was found at the *C1_2_5* locus around 22.1 kb centromeric to the *HLA-Cw* locus, we examined the EHH pattern from the landmark of two-locus haplotype extended from *C1_2_5* to either *HLA-B* or *-Cw* locus. The degree of EHH decay from the haplotypes of *HLA-B* or *-Cw* coupled with *C1_2_5* showed a similar tendency to that obtained from the landmark of *HLA-B* or *-Cw* alone. Interestingly, it was found that the EHH pattern was different between *Cw*0702* and *Cw*0303* even though these two *HLA-Cw* alleles were linked to the identical allele, *C1_2_5*200* (Figure 1d). As expected, the EHH scores of *HLA-Cw/-B* haplotypes tended to maintain a long-range LD extending centromeric and teromeric to the landmark locus (Figure 1e). These observations suggested that the diversity of *C1_2_5* locus at the nucleotide level was well correlated with the lineage of the *HLA-Cw/-B* haplotype.

Structural analysis of *C1_2_5* marker

To further delineate the haplotypic structure of the *HLA-Cw/-B* region, we focused on the motif structure of a microsatellite marker, *C1_2_5*, which was located between *HLA-B* and *HLA-Cw*. Sequencing analysis of *C1_2_5* revealed four motifs consisting of nucleotide substitutions in addition to gain or loss of CA repeat units (Figure 2a). These substitutions *per se* were observed within the repeat tract and hence did not change the size of PCR fragments, whereas the differences of the motif structure provided us with the additional information on diversity, as exemplified by *C1_2_5*200* and *C1_2_5*218*. Using these data, genetic associations between *C1_2_5* alleles and individual *HLA-Cw/-B* alleles were investigated to characterize the diversity of HLA haplotypes. The $(CA)_nCTCA$ and $(CA)_4AA(CA)_5AA(CA)_nCTCA$ motifs were in tight LD with *Cw*0801* and *Cw*0102*, respectively, and the majority of *C1_2_5* alleles showed strong LD, with particularly *HLA-Cw* alleles, but there were several exceptions. For example, *Cw*0304* was in LD with three different *C1_2_5* variations, $(CA)_4AA(CA)_{19}CTCA$, $(CA)_4AA(CA)_{21}CTCA$ and $(CA)_4AA(CA)_{23}TACACTCA$. The former two variations forming the identical *HLA-Cw/-B* haplotype, *Cw*0304-B*4002*, should be derived from the same repeat motif. In contrast, the third variation with different motif was linked to a different HLA-B allele, *B*4001*, forming the *Cw*0304-B*4001* haplotype.

Phylogenetic relationship between alleles of *C1_2_5* and *HLA-Cw*

The mutation rate of SNP was estimated to be 10^{-8} per generation, whereas that of microsatellite was between 10^{-5} and 10^{-3} per generation.[27] Relationships among *C1_2_5* alleles with four motifs were phylogenetically analyzed (Figure 2a). Of four major motifs, the simplest structure was $(CA)_nCTCA$, observed in short alleles of both *C1_2_5*188* and **192*. All other *C1_2_5* alleles had a (CA) to (AA) change at the fifth CA unit, resulting in a motif sequences $(CA)_4\underline{AA}(CA)_n$, interrupting the CA repeat array. In addition, *C1_2_5* alleles containing the interrupting sequence, $(CA)_4AA(CA)_n$, can be subdivided into two different motifs as follows; $(CA)_4AA(CA)_n\underline{TACACTCA}$ resulted from a (CA) to (TA) change in 3'-side of the CA repeat and $(CA)_4AA(CA)_5\underline{AA}(CA)_nCTCA$ resulted from CA-to-AA change at the 11th unit. As all microsatellite motifs shared the simplest motif, it was assumed that $(CA)_nCTCA$ was the core structure of the *C1_2_5* microsatellite. On the other hand, to investigate the relationships of lineage between the *C1_2_5* motif structures and the neighboring SNPs, we constructed a phylogenetic tree using the exon 4 sequences of *HLA-Cw* alleles, which encoded the α3 domain, to exclude the effects of selective pressure acting on the peptide-binding domain (Figure 2b). It was found that the relationship among *C1_2_5* alleles (microsatellite lineage) was not always concordant with the relationship of *HLA-Cw* alleles (SNPs lineage).

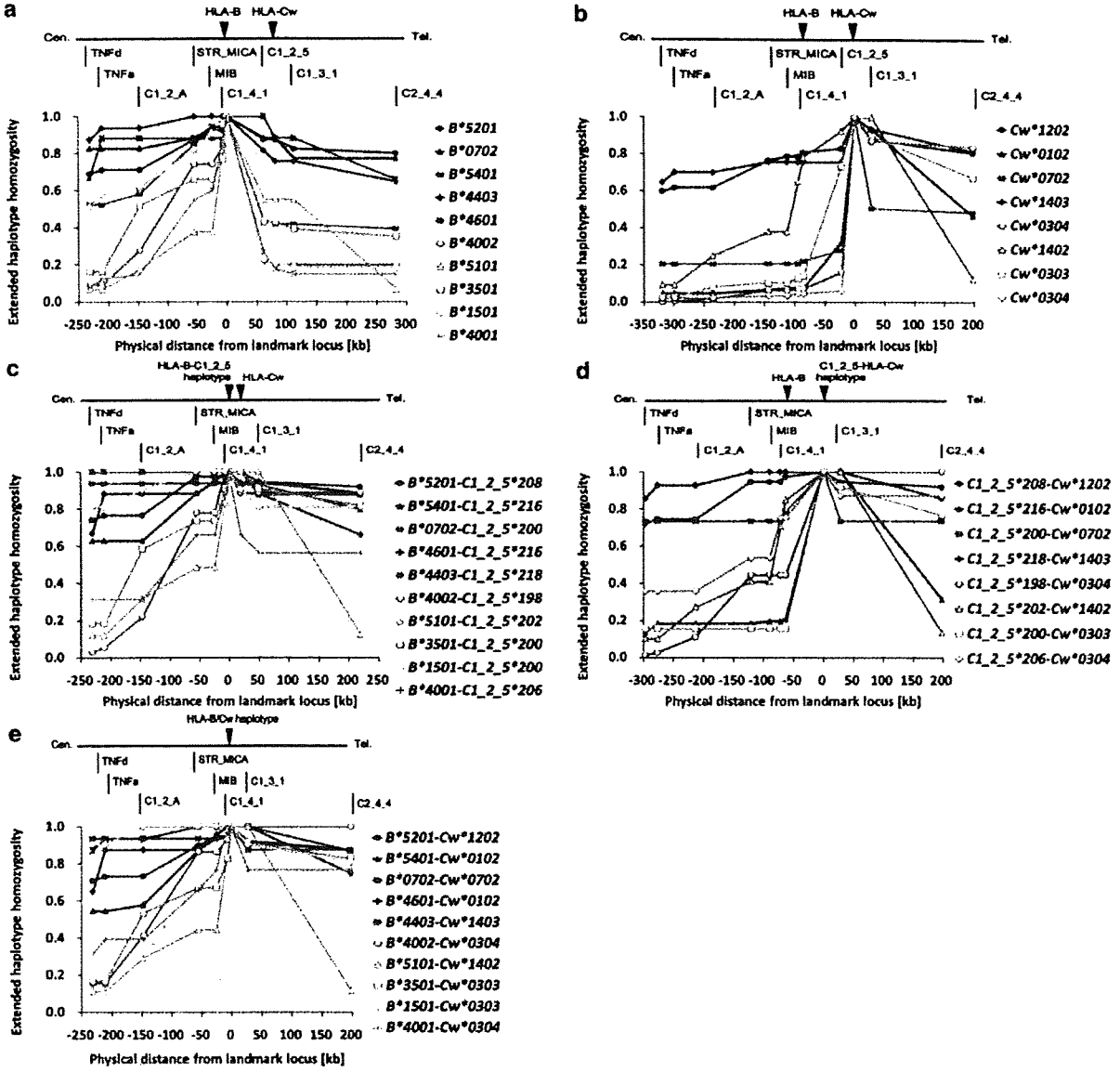

Figure 1 Long-range haplotype test using classical *HLA* genes and microsatellite markers. Each plot represents the extended haplotype homozygosity (EHH) values spanning about 200–300 kb from alleles at two landmark loci, (**a**) *HLA-B* and (**b**) *HLA-Cw*, and three two-locus haplotypes, (**c**) *HLA-B-C_1_2_5*, (**d**) *C1_2_5-HLA-Cw* and (**e**) *HLA-B-HLA-Cw*, in both directions. Vertical lines and arrowheads over the map indicate the locations of microsatellite markers and *HLA* loci, respectively. The gene map was obtained from the Wellcome Trust Sanger Institute (http://www.sanger.ac.uk/HGP/Chr6/MHC.shtml). The physical distances are given in kb, with negative and positive numbers used for locations proximal to and distal from the landmark, respectively.

Multiallelic analysis of LD between *C1_2_5* and its franking *HLA* genes

As the EHH analysis was focused on the LD among specific pairs of alleles and haplotypes with relatively high frequency (>3%), we also evaluated overall LDs between two loci among *HLA-B*, *-Cw* and *C1_2_5* to figure out the overall nature of the LD structure in this region (Table 3). It was found that the *C1_2_5* locus, at both the allele level and the motif level, showed stronger LD with *HLA-Cw/-B* haplotype than with either *HLA-B* or *-Cw* locus. These observations suggested that the divergence of *C1_2_5* locus reflected its tight association with the *HLA-Cw/-B* haplotype rather than the association with *HLA-Cw* alleles or *HLA-B* alleles.

DISCUSSION

In this study, we investigated whether a microsatellite marker adjacent to the most polymorphic *HLA-Cw/-B* loci could provide us with information to delineate the haplotype lineage. We found that the *C1_2_5* microsatellite was highly variable by three substitutions within the CA repeat array in addition to the number of CA repeats. The unique polymorphic patterns at *C1_2_5* locus were well correlated with the *HLA-Cw/-B* haplotypes. It was also shown that the simple analysis of fragment-size variation should overlook the nature of microsatellite variations.

The structure of repeat motif was attractive from the evolutional viewpoint because the microsatellite and *HLA-Cw* alleles appeared to

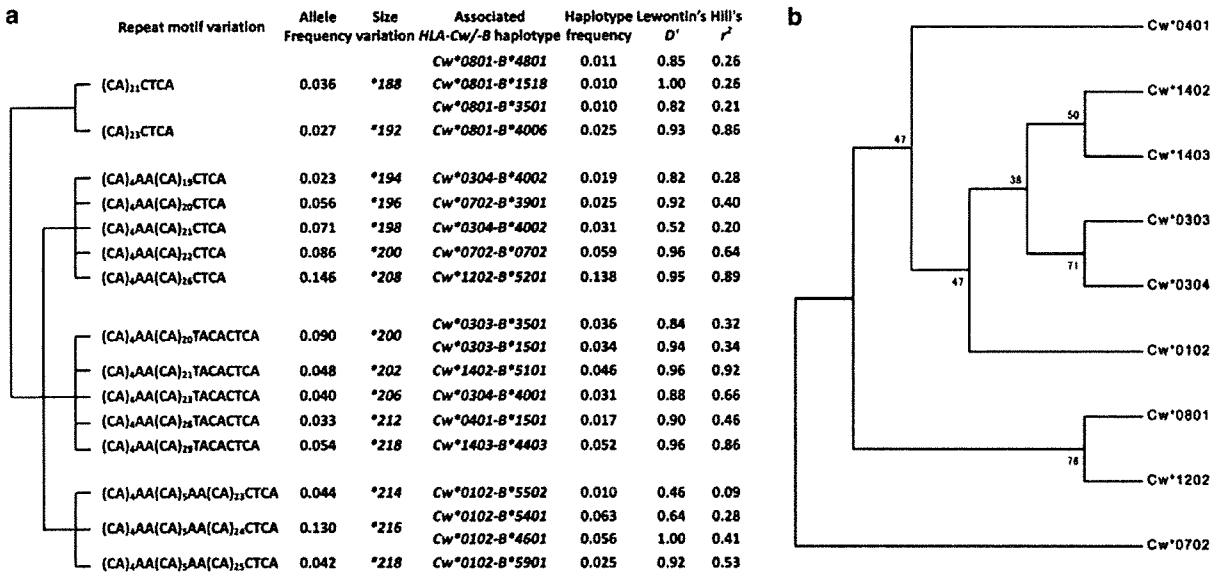

Figure 2 Phylogenetic relationship between *C1_2_5* motif and *HLA-Cw/-B* haplotype. (**a**) Phylogenetic tree predicted from the repeat motif structures at the *C1_2_5* locus. *HLA-Cw/-B* haplotypes associated with *C1_2_5* alleles were indicated with two LD coefficients, *D'* and r^2. Representative *HLA-B* alleles were shown. (**b**) Phylogenetic analysis of exon 4 sequences of *HLA-Cw*. Phylogenetic tree was constructed by the UPGMA method. The numbers for interior branches refer to the bootstrap values in percentage with 1000 replications.

Table 3 Overall LD among *HLA-B*, *HLA-Cw* and *C1_2_5* loci

LD pair[a]	*Hedrick's multiallelic D'*	*Cramer's V*
HLA-B locus and C1_2_5 locus	0.85	0.70
HLA-B locus and C1_2_5 motif	0.88	0.60
C1_2_5 locus and HLA-Cw locus	0.87	0.64
C1_2_5 motif and HLA-Cw locus	0.91	0.73
HLA-Cw locus and HLA -B locus	0.88	0.82
HLA-Cw/-B haplotype and C1_2_5 locus	0.94	0.85
HLA-Cw/-B haplotype and C1_2_5 motif	0.95	0.74

Overall LDs for each pair were statistically significant ($P<0.05$).
[a]C1_2_5 locus and C1_2_5 motif indicate allele (fragment size) and repeat motif structure, respectively.

co-evolve. For example, the change of *C1_2_5* found in the *Cw*0304-B*4002* haplotypes was attributable to the differences in the number of repetitive units, which can be explained by a strand-slippage mechanism. On the other hand, the difference of repeat motifs in *C1_2_5*198* and *C1_2_5*206* associated with the identical allele, *Cw*0304*, was characterized by distinct *HLA-B* alleles, *B*4002* and *B*4001*, respectively. It was unlikely that these two *Cw*0304*-linked haplotypes were shaped by a simple recombination event between *HLA-Cw* and *-B* loci, as the motif structures of *C1_2_5* were different between them. Instead, *Cw*0304* might originally exist in two different haplotype lineages.

Comparison of EHH profile showed that the length of LD varied depending on the HLA haplotypes. One possible explanation for the variation includes the diversity of pairing between the alleles of *HLA-B* and *-Cw*. Indeed, the *HLA* allele with a short-range LD profile showed larger diversity due to the repeated recombination events over time, thereby providing the LD decay between the landmark allele and the linked markers. On the other hand, haplotypes with a long-range LD profile might be of recent origin. In general, human genetic geography showed high continuity, and it is well known that the MHC haplotypes in neighboring populations were introduced to Japan through multiple routes.[28] Therefore, the MHC haplotype structures in the Japanese population might be shaped by multiple immigrations.

Each repeat motif observed in the *C1_2_5* locus was in tight LD with a particular *HLA-Cw* allele and in part with an *HLA-B* allele, which consisted of *HLA-Cw/-B* haplotypes. The mutation rate at a microsatellite is known to depend on the intrinsic features, including repeat number, length and motif size.[29] For example, microsatellites with greater number of repeats showed higher mutation rates due to the increased probability of slippage.[30] In contrast, interruption of perfect repeat array had a great impact on the stability of microsatellite alleles.[31] Indeed, interrupted motif within repeat tracts that were correlated with *HLA-DR/-DQ* haplotypes was described for *DQCAR*.[32]

In conclusion, we revealed that unique mutational dynamics at *C1_2_5* locus could serve as a useful resource for tracing haplotype lineage in the Japanese population. Analysis of *C1_2_5* structures along with *HLA-Cw/-B* haplotypes in other ethnic groups will show the lineages of haplotypes. Statistical methodology for predicting the *HLA* allele and its haplotype carried on the chromosome have been established using informative SNPs inside and/or outside the *HLA* genes.[33,34] However, the use of bi-allelic SNPs as a marker requires more efforts to obtain the information than the use of multi-allelic microsatellite markers, because many *HLA* alleles show a mosaic structure shaped by multiple polymorphic backgrounds. Microsatellite markers will shed light on the haplotype lineage in a different perspective from the SNP-based tagging approach.

ACKNOWLEDGEMENTS

We are grateful to Atsuko Shigenari, Eri F Kikkawa, Hisako Kawata, Norihisa Sugita, Daisuke Sumiyama, Ryoko Ohkubo, Rui-Ping Dong, Shuji Hoshino, Masayuki Yoshida, Shin-ichiro Yasunaga and Yukiji Date for their contributions

in genotyping. This work was supported in part by Grant-in-Aids from the Ministry of Education, Science, Sports, Culture and Technology (MEXT) of Japan, the program of Founding Research Centers for Emerging and Reemerging Infection Disease supported by MEXT, Japan, and research grants from the Ministry of Health, Labor and Welfare, Japan, and from the Japan Health Sciences Foundation.

1 Horton, R., Wilming, L., Rand, V., Lovering, R. C., Bruford, E. A., Khodiyar, V. K. *et al.* Gene map of the extended human MHC. *Nat. Rev. Genet.* **5,** 889–899 (2004).
2 Cooke, G. S. & Hill, A. V. Genetics of susceptibility to human infectious disease. *Nat. Rev. Genet.* **2,** 967–977 (2001).
3 Rudolph, M. G., Stanfield, R. L. & Wilson, I. A. How TCRs bind MHCs, peptides, and coreceptors. *Annu. Rev. Immunol.* **24,** 419–466 (2006).
4 Little, A. M. & Parham, P. Polymorphism and evolution of HLA class I and II genes and molecules. *Rev. Immunogenet.* **1,** 105–123 (1999).
5 Meyer, D., Single, R. M., Mack, S. J., Erlich, H. A. & Thomson, G. Signatures of demographic history and natural selection in the human major histocompatibility complex loci. *Genetics.* **173,** 2121–2142 (2006).
6 Miretti, M. M., Walsh, E. C., Ke, X., Delgado, M., Griffiths, M., Hunt, S. *et al.* A high-resolution linkage-disequilibrium map of the human major histocompatibility complex and first generation of tag single-nucleotide polymorphisms. *Am. J. Hum. Genet.* **76,** 634–646 (2005).
7 Shichi, D., Kikkawa, E. F., Ota, M., Katsuyama, Y., Kimura, A., Matsumori, A. *et al.* The haplotype block, NFKBIL1-ATP6V1G2-BAT1-MICB-MICA, within the class III-class I boundary region of the human major histocompatibility complex may control susceptibility to hepatitis C virus-associated dilated cardiomyopathy. *Tissue Antigens* **66,** 200–208 (2005).
8 Shiina, T., Ota, M., Shimizu, S., Katsuyama, Y., Hashimoto, N., Takasu, M. *et al.* Rapid evolution of major histocompatibility complex class I genes in primates generates new disease alleles in humans via hitchhiking diversity. *Genetics* **173,** 1555–1570 (2006).
9 Ahmad, T., Neville, M., Marshall, S. E., Armuzzi, A., Mulcahy-Hawes, K., Crawshaw, J. *et al.* Haplotype-specific linkage disequilibrium patterns define the genetic topography of the human MHC. *Hum. Mol. Genet.* **12,** 647–656 (2003).
10 Horton, R., Gibson, R., Coggill, P., Miretti, M., Allcock, R. J., Almeida, J. *et al.* Variation analysis and gene annotation of eight MHC haplotypes: the MHC Haplotype Project. *Immunogenetics* **60,** 1–18 (2008).
11 Nagy, M., Entz, P., Otremba, P., Schoenemann, C., Murphy, N. & Dapprich, J. Haplotype-specific extraction: a universal method to resolve ambiguous genotypes and detect new alleles—demonstrated on HLA-B. *Tissue Antigens* **69,** 176–180 (2007).
12 Subirana, J. A. & Messeguer, X. Structural families of genomic microsatellites. *Gene* **408,** 124–132 (2008).
13 Matsuzaka, Y., Makino, S., Nakajima, K., Tomizawa, M., Oka, A., Bahram, S. *et al.* New polymorphic microsatellite markers in the human MHC class III region. *Tissue Antigens* **57,** 397–404 (2001).
14 Matsuzaka, Y., Makino, S., Nakajima, K., Tomizawa, M., Oka, A., Kimura, M. *et al.* New polymorphic microsatellite markers in the human MHC class II region. *Tissue Antigens* **56,** 492–500 (2000).
15 Foissac, A., Salhi, M. & Cambon-Thomsen, A. Microsatellites in the HLA region: 1999 update. *Tissue Antigens* **55,** 477–509 (2000).
16 Cullen, M., Malasky, M., Harding, A. & Carrington, M. High-density map of short tandem repeats across the human major histocompatibility complex. *Immunogenetics* **54,** 900–910 (2003).
17 Malkki, M., Single, R., Carrington, M., Thomson, G. & Petersdorf, E. MHC microsatellite diversity and linkage disequilibrium among common HLA-A, HLA-B, DRB1 haplotypes: implications for unrelated donor hematopoietic transplantation and disease association studies. *Tissue Antigens* **66,** 114–124 (2005).
18 Mungall, A. J., Palmer, S. A., Sims, S. K., Edwards, C. A., Ashurst, J. L., Wilming, L. *et al.* The DNA sequence and analysis of human chromosome 6. *Nature* **425,** 805–811 (2003).
19 Saito, S., Ota, S., Yamada, E., Inoko, H. & Ota, M. Allele frequencies and haplotypic associations defined by allelic DNA typing at HLA class I and class II loci in the Japanese population. *Tissue Antigens* **56,** 522–529 (2000).
20 Stewart, C. A., Horton, R., Allcock, R. J., Ashurst, J. L., Atrazhev, A. M., Coggill, P. *et al.* Complete MHC haplotype sequencing for common disease gene mapping. *Genome Res.* **14,** 1176–1187 (2004).
21 Lancaster, A. K., Single, R. M., Solberg, O. D., Nelson, M. P. & Thomson, G. PyPop update-software pipeline for large-scale multilocus population genomics. *Tissue Antigens* **69**(Suppl 1), 192–197 (2007).
22 Warnes, G. R. The genetics package. *R News* **3,** 9–13 (2003).
23 Schaid, D. J., Rowland, C. M., Tines, D. E., Jacobson, R. M. & Poland, G. A. Score tests for association between traits and haplotypes when linkage phase is ambiguous. *Am. J. Hum. Genet.* **70,** 425–434 (2002).
24 Sabeti, P. C., Reich, D. E., Higgins, J. M., Levine, H. Z., Richter, D. J., Schaffner, S. F. *et al.* Detecting recent positive selection in the human genome from haplotype structure. *Nature* **419,** 832–837 (2002).
25 Hedrick, P. W. Gametic disequilibrium measures: proceed with caution. *Genetics* **117,** 331–341 (1987).
26 Cramer, H. *Mathematical Methods of Statistics* (Princeton University Press, Princeton, New Jersey, 1946).
27 Lander, E. S., Linton, L. M., Birren, B., Nusbaum, C., Zody, M. C., Baldwin, J. *et al.* Initial sequencing and analysis of the human genome. *Nature* **409,** 860–921 (2001).
28 Tokunaga, K., Ishikawa, Y., Ogawa, A., Wang, H., Mitsunaga, S., Moriyama, S. *et al.* Sequence-based association analysis of HLA class I and II alleles in Japanese supports conservation of common haplotypes. *Immunogenetics* **46,** 199–205 (1997).
29 Ellegren, H. Microsatellites: simple sequences with complex evolution. *Nat. Rev. Genet.* **5,** 435–445 (2004).
30 Lai, Y. & Sun, F. The relationship between microsatellite slippage mutation rate and the number of repeat units. *Mol. Biol. Evol.* **20,** 2123–2131 (2003).
31 Boyer, J. C., Hawk, J. D., Stefanovic, L. & Farber, R. A. Sequence-dependent effect of interruptions on microsatellite mutation rate in mismatch repair-deficient human cells. *Mutat. Res.* **640,** 89–96 (2008).
32 Macaubas, C., Jin, L., Hallmayer, J., Kimura, A. & Mignot, E. The complex mutation pattern of a microsatellite. *Genome Res.* **7,** 635–641 (1997).
33 Leslie, S., Donnelly, P. & McVean, G. A Statistical method for predicting classical HLA alleles from SNP data. *Am. J. Hum. Genet.* **82,** 48–56 (2008).
34 de Bakker, P. I., McVean, G., Sabeti, P. C., Miretti, M. M., Green, T., Marchini, J. *et al.* A high-resolution HLA and SNP haplotype map for disease association studies in the extended human MHC. *Nat. Genet.* **38,** 1166–1172 (2006).

Impact of novel TRIM5α variants, Gly110Arg and G176del, on the anti-HIV-1 activity and the susceptibility to HIV-1 infection

Toshiaki Nakajima[a,b,*], Emi E. Nakayama[c,*], Gurvinder Kaur[d], Hiroshi Terunuma[e], Jun-ich Mimaya[f], Hitoshi Ohtani[a,b], Narinder Mehra[d], Tatsuo Shioda[c] and Akinori Kimura[a,b]

Objective: TRIM5α is one of the factors contributing to intracellular defense mechanisms against HIV-1 infection. We investigated the association of TRIM5α sequence variations with the susceptibility to HIV-1 infection in Japanese and Indian.

Design: Sequence variations in TRIM5α were investigated in HIV-1-infected patients and ethnic-matched controls. Functional alterations caused by rare variants were analyzed.

Methods: We sequenced TRIM5α-exon 2 in both Japanese (94 HIV-1-infected patients and 487 controls) and Indian (101 HIV-1-infected patients and 99 controls). Frequency of variants and haplotypes were compared between the HIV-1-infected patients and controls. Functional analyses were performed for two rare variants, Gly110Arg and G176del.

Results: The frequency of 43Tyr-allele in the Indian HIV-1-infected patients was significantly lower than that in the ethnic-matched controls (odds ratio = 0.52, 95% confidence interval = 0.31–0.89, $P = 0.015$). A similar tendency was observed in Japanese sample, although it was not statistically significant (odds ratio = 0.67, 95% confidence interval = 0.43–1.05, $P = 0.095$). On the other hand, haplotype analyses revealed that the haplotype carrying the 43Tyr-allele was significantly associated with the reduced susceptibility to HIV-1 infection in both ethnic groups. Functional analysis revealed that Gly110Arg variant weakened the anti-HIV-1 and anti-HIV-2 activities of human TRIM5α, whereas the truncated G176del-TRIM5 enhanced the antiviral activity of coexpressed TRIM5α. Epidemiological data were consistent in that Gly110Arg and G176del were associated with the susceptibility to and protection from HIV-1 infection, respectively.

Conclusion: Both common and rare variants of TRIM5α are associated with the susceptibility to HIV-1 infection.

AIDS 2009, **23**:000–000

Keywords: association, HIV-1, polymorphism, susceptibility, TRIM5

[a]Department of Molecular Pathogenesis, Medical Research Institute, [b]Laboratory of Genome Diversity, Graduate School of Biomedical Science, Tokyo Medical and Dental University, Tokyo, [c]Department of Viral Infection, Research Institute for Microbial Disease, Osaka University, Osaka, Japan, [d]Department of Transplant Immunology and Immunogenetics, All India Institute of Medical Sciences, New Delhi, India, [e]Biotherapy Institute of Japan, Tokyo, and [f]Division of Hematology and Oncology, Shizuoka Children's Hospital, Shizuoka, Japan.

Correspondence to Akinori Kimura, MD, PhD, Department of Molecular Pathogenesis, Medical Research Institute, Tokyo Medical and Dental University, 1-5-45 Yushima, Bunkyo-ku, Tokyo 113-8510, Japan.

Tel: +81 3 5803 4905; fax: +81 3 5803 4907; e-mail: akitis@mri.tmd.ac.jp

*T.N. and E.E.N. contributed equally to this study.

Received: 25 March 2009; revised: 22 July 2009; accepted: 29 July 2009.

DOI:10.1097/QAD.0b013e328331567a

ISSN 0269-9370 © 2009 Wolters Kluwer Health | Lippincott Williams & Wilkins

Introduction

Although the cellular and humoral immune systems are known to play crucial roles in the defense against retroviral infection, mammals have also evolved defense mechanisms within cells. Several lines of evidence indicated that restriction factors within host cells inhibit viral replication more effectively than the immune system, and TRIM5α is one of the factors involved in the intracellular defense against retroviruses [1,2]. It was reported that TRIM5α from rhesus monkeys restricted HIV-1 production at a postentry, preintegration stage in the viral life cycle through rapid degradation of HIV-1 Gag polyproteins [3,4], whereas human TRIM5α restricted HIV-1 only weakly and potently restricted N-tropic murine leukemia virus [5,6].

TRIM5 is a member of the tripartite-motif containing superfamily and includes a Really Interesting New Gene (RING) domain, B-box 2 domain and coiled-coil domain [7]. Alternative splicing of TRIM5 gene generates several isoforms of TRIM5 proteins. One isoform, TRIM5α, contains the carboxy-terminal B30.2 (SPRY) domain that is essential for anti-HIV-1 activity, and sequence differences in the SPRY domain contribute to the differences in the anti-HIV-1 activity among primate species [4,8–13].

It is well known that the infection by HIV-1 and progression to AIDS are variable among human individuals, which are considered to be controlled by diversity in the human genome [14,15]. As TRIM5α has crucial roles in the restriction of viral replication within the host cells, it is a good candidate gene controlling the susceptibility to or protection from HIV-1 infection and/or progression to AIDS. Actually, several studies have demonstrated that common TRIM5α functional polymorphisms, His43Tyr and Arg136Gln, were associated with the susceptibility to HIV-1 infection. However, the significance of association has not been established [16–20].

In this study, we investigated two ethnic populations, Japanese and Indian, for the polymorphism in TRIM5α-exon 2 and its association with the HIV-1 infection. We found that a TRIM5α haplotype carrying the 43Tyr-allele was associated with the reduced susceptibility to HIV-1 infection in both ethnic groups. In addition, we identified two rare variants, G176del and Gly110Arg, which affected the anti-HIV-1 activity and showed suggestive associations with the HIV-1 infection.

Material and methods

Participants

Protocol of the present study was approved by the Ethics Review Board of the Medical Research Institute, Tokyo Medical and Dental University and that of All India Institute of Medical Science. At the set-up of the cohort in 1995, all the HIV-1-infected Japanese hemophiliac patients had been infected for longer than 10 years and they were asymptomatic without any antiviral measures. Blood samples were collected from 94 well characterized patients who were selected from the cohort after obtaining written informed consent [21,22]. Control DNA samples were prepared from Epstein–Barr virus-transformed human B cell lines established from randomly selected healthy donors with written informed consent ($n = 487$), which were purchased from the Japan Health Sciences Foundation. The DNA samples from HIV-1-infected individuals were prepared from the blood sample by using QuickGene DNA whole blood kit S (FUJIFILM, Tokyo, Japan). In addition, blood DNA samples were obtained with written informed consent from 101 HIV-1-infected Indian patients and 99 healthy Indian volunteers in the related hospitals of All India Institute of Medical Sciences, New Delhi. DNA samples from whites ($n = 96$) and African–Americans ($n = 96$) were obtained from the Coriell Institute for Medical Research (Camden, New Jersey, USA).

Identification and genotyping of nucleotide variations in TRIM5α-exon 2

Primer sets were designed to amplify the genomic segments covering the entire TRIM5α-exon 2 as follows: sense primer (5′-TTGGTCCCATTTTAACC TTCC-3′) and antisense primer (5′-AAGGCAGT TAA TGTCAAAGGC-3′). Genomic DNA was subjected to PCR amplification followed by sequencing on both strands using the BigDye Terminator v3.1 Cycle Sequencing Kit (Applied Biosystems, Foster City, California, USA). Polymorphisms were identified using the Sequencher program (Gene Code Co., Ann Arbor, Michigan, USA).

Cloning and expression of TRIM5α

The generation of recombinant Sendai viruses (SeVs) expressing human TRIM5α, human/African green monkey (AGM) chimeric TRIM5α [18], cynomolgus monkey TRIM5α lacking SPRY domain [CM-TRIM5α-SPRY(−)-HA] [23] and AGM TRIM5α lacking coiled-coil domain [AGM-TRIM5α-CC(−)-HA] has been described previously [24]. All TRIM5α variants carried a hemagglutinin (HA)-tag (YPYDVP-DYAA) at the C-terminus. The Gly110Arg mutation was introduced into both human TRIM5α and human/AGM chimeric TRIM5α by PCR site-directed mutagenesis. To generate SeV expressing G176del carrying an HA-tag at the N-terminus (HA-G176del-TRIM5), the amplified PCR fragment from genomic DNA carrying G176del was cloned into a pSeV18+b(+) vector. Recombinant SeVs expressing human 110Arg-TRIM5α, human/AGM chimeric 110Arg-TRIM5α and HA-G176del-TRIM5 were recovered as described previously [12]. The second passages in embryonated

chicken eggs were used as the stock viruses in all experiments.

Western blot analysis

MT4 cells (1×10^6) infected with recombinant SeVs expressing HA-tagged TRIM5α proteins were lysed in lysis buffer (50 mmol/l Tris-HCl, pH 7.5, 150 mmol/l NaCl, 1% Nonidet P40, 0.5% sodium deoxycholate). Western blot analyses with anti-HA high-affinity rat monoclonal antibody (Roche, Indianapolis, Indiana, USA) and anti-CypA affinity rabbit polyclonal antibody (Sigma, St Louis, Missouri, USA) were performed as described previously [19].

Viral infection

MT4 or CEM-SS cells (1×10^5) were infected with SeV expressing human TRIM5α, human 110Arg-TRIM5α, human/AGM chimeric TRIM5α, human/AGM chimeric 110Arg-TRIM5α, CM-TRIM5α-SPRY(−) or AGM-TRIM5α-CC(−) at a multiplicity of infection of 10 plaque-forming units (PFUs) per cell and incubated at 37°C for 9 h. To examine the effects of G176del-TRIM5 on the full length TRIM5α, 5 PFU per cell of each SeV expressing either CM-TRIM5α-SPRY(−), AGM-TRIM5α-CC(−) or HA-G176del-TRIM5 was simultaneously inoculated to MT4 cells with SeV expressing human/AGM chimeric TRIM5α. Cells were then superinfected with 30 ng of p24 of an X4 HIV-1 strain NL43 or 30 ng of p25 of HIV-2 GH123. The culture supernatants were collected periodically and the level of p24 or p25 was measured by RETROtek antigen ELISA kit (ZeptoMetrix, Buffalo, New York, USA).

Statistical analysis

All statistical analyses in this study were performed using GraphPad InStat version 3.06 for Windows (GraphPad Software, San Diego, California, USA). Correction for multiple testing was done by multiplying the P value by the number of tested markers to obtain the corrected P (P_c) value. Haplotype association analyses were performed by using SNPAlyze version 6.0 standard (DYNACOM Co., Ltd., Tokyo, Japan). Meta-analysis was performed using a Mantel–Haenszel method. P values less than 0.05 were considered to be statistically significant.

Results

Associations of TRIM5α-exon 2 polymorphism with susceptibility to HIV-1 infection

We identified 10 different nucleotide variations in the TRIM5α-exon 2 in this study and eight of them were reported in previous studies. Most of the sequence variations, except for His43Tyr, Val112Phe and Arg136Gln were observed with low frequencies (allele frequency less than 0.05) in the tested populations. Associations between the TRIM5α polymorphisms and the susceptibility to HIV-1 infection were summarized in Table 1. The frequency of 43Tyr-allele in Indian HIV-1-infected patients was significantly lower than that in the ethnic-matched controls [odds ratio (OR) (95% confidence interval (CI)) = 0.52 (0.31–0.89), $P = 0.015$ by χ^2 test]. A similar tendency was observed in Japanese, although it did not reach statistical significance [OR (95% CI) = 0.67 (0.43–1.05), $P = 0.095$ by χ^2 test]. A meta-analysis of data from two populations demonstrated the significant association corrected for multiple testing [OR (95% CI) = 0.61 (0.43–0.85), $P = 0.0004$, $P_c = 0.004$]. When we analyzed the data for HIV-1 loads after 7–8 years during the observation period, which were available for 75 Japanese HIV-1-infected patients, no significant correlation between the His43Tyr genotype and HIV-1 loads was observed (data not shown).

Two novel polymorphisms, Gly110Arg and G176del, were identified only in the Japanese samples. The Gly110Arg variant was more frequent in the HIV-1-infected patients than in the controls [OR (95% CI) = 13.12 (2.53–68.21), $P = 0.002$ by Fisher's exact test]. On the other hand, the G176del variant, a deletion of a G at the coding nucleotide position 176 from the initiation site of translation, which may result in a truncated TRIM5 protein product, was found only in the Japanese controls.

TRIM5α haplotype and susceptibility to HIV-1 infection

The associations between the susceptibility to HIV-1 infection and TRIM5α haplotypes composed of five sequence variations with relatively high frequency, His43Tyr, Gly110Arg, Val112Phe, Thr128Thr and Arg136Gln, were investigated in Japanese and Indian populations (Table 2). In both populations, the frequency of a common haplotype 43Tyr-110Gly-112Val-128Thr-136Arg was significantly low in the HIV-1-infected patients. This result was consistent with the association of 43Tyr with the reduced susceptibility to HIV-1 infection, because this haplotype was in tight linkage disequilibrium with the 43Tyr-allele.

Anti-HIV-1 activity of TRIM5α was attenuated by Gly110Arg substitution

To investigate the functional significance of Gly110Arg on the anti-HIV activity of TRIM5α, we constructed a SeV containing a C-terminal HA-tagged human 110Arg-TRIM5α (Fig. 1a). As shown in Fig. 1b, expression level of variant 110Arg-TRIM5α was comparable to that of wild-type human TRIM5α. A human/AGM chimeric TRIM5α, which possessed the SPRY domain of AGM TRIM5α, was also generated to enhance the weak anti-HIV-1 activity of human TRIM5α (Fig. 1a). As shown in Fig. 1b, the expression level of human/AGM chimeric

Table 1. Allele frequencies of TRIM5α-exon 2 sequence variations and associations of them with HIV-1/AIDS susceptibility.

	Japanese			Indian			White	African–American
Sequence variations[a]	Control ($n=487$)	HIV-1-infected patients ($n=94$)	Odds ratio (95% confidence interval)	Control ($n=99$)	HIV-1-infected patients ($n=101$)	Odds ratio (95% confidence interval)	Control ($n=96$)	Control ($n=96$)
Gly31Ser	0.000	0.000	ND	0.000	0.000	ND	0.000	0.032
His43Tyr	0.184	0.133	0.67 (0.42 – 1.05)	0.227	0.134****	0.52 (0.31 – 0.89)	0.115	0.068
Cys58Tyr	0.000	0.000	ND	0.000	0.000	ND	0.000	0.011
G176del	0.005	0.000	ND	0.000	0.000	ND	0.000	0.000
Asp109Asp	0.000	0.000	ND	0.000	0.000	ND	0.000	0.005
Gly110Arg	0.002	0.021***	13.14 (2.53 – 68.21)	0.000	0.000	ND	0.000	0.000
Gly110Glu	0.000	0.000	ND	0.000	0.000	ND	0.005	0.005
Val112Phe	0.052	0.043	0.80 (0.37 – 1.70)	0.192	0.198	1.04 (0.63 – 1.71)	0.052	0.021
Thr128Thr	0.000	0.011**	ND	0.000	0.000	ND	0.000	0.000
Arg136Gln	0.105	0.144	1.48 (0.94 – 2.32)	0.177	0.173	0.98 (0.58 – 1.64)	0.349	0.177

ND, not defined.
[a]The numbers of sequence variations, except for G176del, are referenced by the amino acid coding position of TRIM5α. G176del is a deletion of a G at the coding nucleotide position 176 from the initiation site of translation.
**$P<0.05$ in Fisher's exact test, when compared with control.
***$P<0.01$ in Fisher's exact test, when compared with control.
****$P<0.05$ in χ^2 test with Yates correction, when compared with control.

Table 2. Haplotype frequencies of four common haplotypes for TRIM5α-exon 2 and association of them with HIV-1/AIDS susceptibility.

	Japanese				Indian			
Haplotype (His43Tyr-Gly110Arg-Val112Phe-Thr128Thr-Arg136Gln)	Control ($n=487$)	HIV-1-infected patients ($n=94$)	P value in permutation test	Odds ratio (95% confidence interval)	Control ($n=99$)	HIV-1-infected patients ($n=101$)	P value in permutation test	Odds ratio (95% confidence interval)
43His-110Gly-112Val-128Thr-136Arg	0.659	0.721	0.129	1.35 (0.96 – 1.91)	0.404	0.495	0.076	1.45 (0.97 – 2.15)
43Tyr-110Gly-112Val-128Thr-136Arg	0.184	0.089	0.001*	0.44 (0.26 – 0.75)	0.227	0.134	0.008*	0.52 (0.31 – 0.89)
43His-110Gly-112Val-128Thr-136Gln	0.103	0.090	0.645	0.87 (0.51 – 1.49)	0.177	0.173	0.909	0.98 (0.58 – 1.64)
43His-110Gly-112Phe-128Thr-136Arg	0.051	0.031	0.251	0.61 (0.26 – 1.44)	0.192	0.198	0.802	1.04 (0.64 – 1.71)

*$P<0.01$ in permutation test.

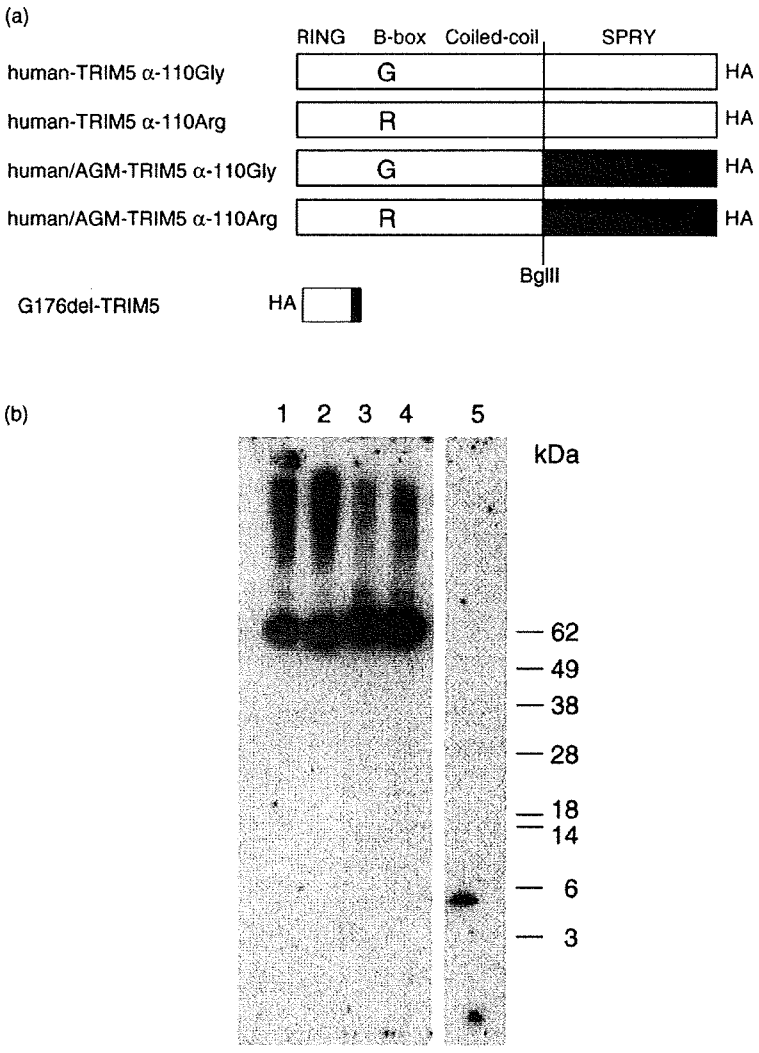

Fig. 1. Expression of TRIM5α constructs used in this study. (a) Schematic representation of TRIM5α fused with a hemaglutinin (HA)-tag. Domain structures of TRIM5α are shown at the top. White and black bars denote human and African green monkey (AGM) sequences, respectively. Gray bar denotes the G176del-specific 16 amino acid residues generated by the frameshift. A BglII site was used to exchange carboxy-terminal B30.2 (SPRY) domains between human and AGM TRIM5α. 'G' or 'R' denotes the amino acid residue at the 110th position. WT denotes wild type. (b) Western blot analysis of TRIM5 protein expressed by recombinant Sendai virus (SeV). MT4 cells were infected with a SeV containing a HA-tagged variant (110Arg) human TRIM5α (lane 1), wild-type human TRIM5α (lane 2), human/AGM chimeric 110Arg-TRIM5α (lane 3), human/AGM chimeric wild-type-TRIM5α (lane 4) and G176del-TRIM5 (lane 5). Sixteen hours after the infection, cells were lysed and subjected to SDS-PAGE. HA-tagged proteins were detected by anti-HA antibody.

110Arg-TRIM5α was similar to that of human/AGM chimeric wild-type-TRIM5α.

These TRIM5α constructs were tested for their ability to restrict the X4-tropic HIV-1 strain NL43 and HIV-2 strain GH123. MT4 cells infected with recombinant SeV expressing each of the TRIM5α constructs were super-infected with HIV-1 NL43 or HIV-2 GH123. We used SeV expressing cynomolgus monkey TRIM5α lacking the SPRY domain CM-TRIM5α-SPRY(−) as a negative control for functional TRIM5α, as overexpression of TRIM5α lacking the SPRY domain exerted a dominant negative effect on the endogenous human TRIM5α [24]. We also used SeV expressing AGM-TRIM5α lacking the coiled-coil domain AGM-TRIM5α-CC(−) as a non-interfering control [24]. As shown in Fig. 2a, both wild-type (110Gly) and variant (110Arg) human/AGM chimeric TRIM5α strongly restricted HIV-1 NL43. On the other hand, both wild-type and variant human TRIM5α showed only weak anti-HIV-1 activity. There was, however, a small increase of HIV-1 in cells expressing the human/AGM chimeric 110Arg-TRIM5α than the cells with the human/AGM chimeric TRIM5α. In the case of HIV-2, virus grew to higher titers in cells

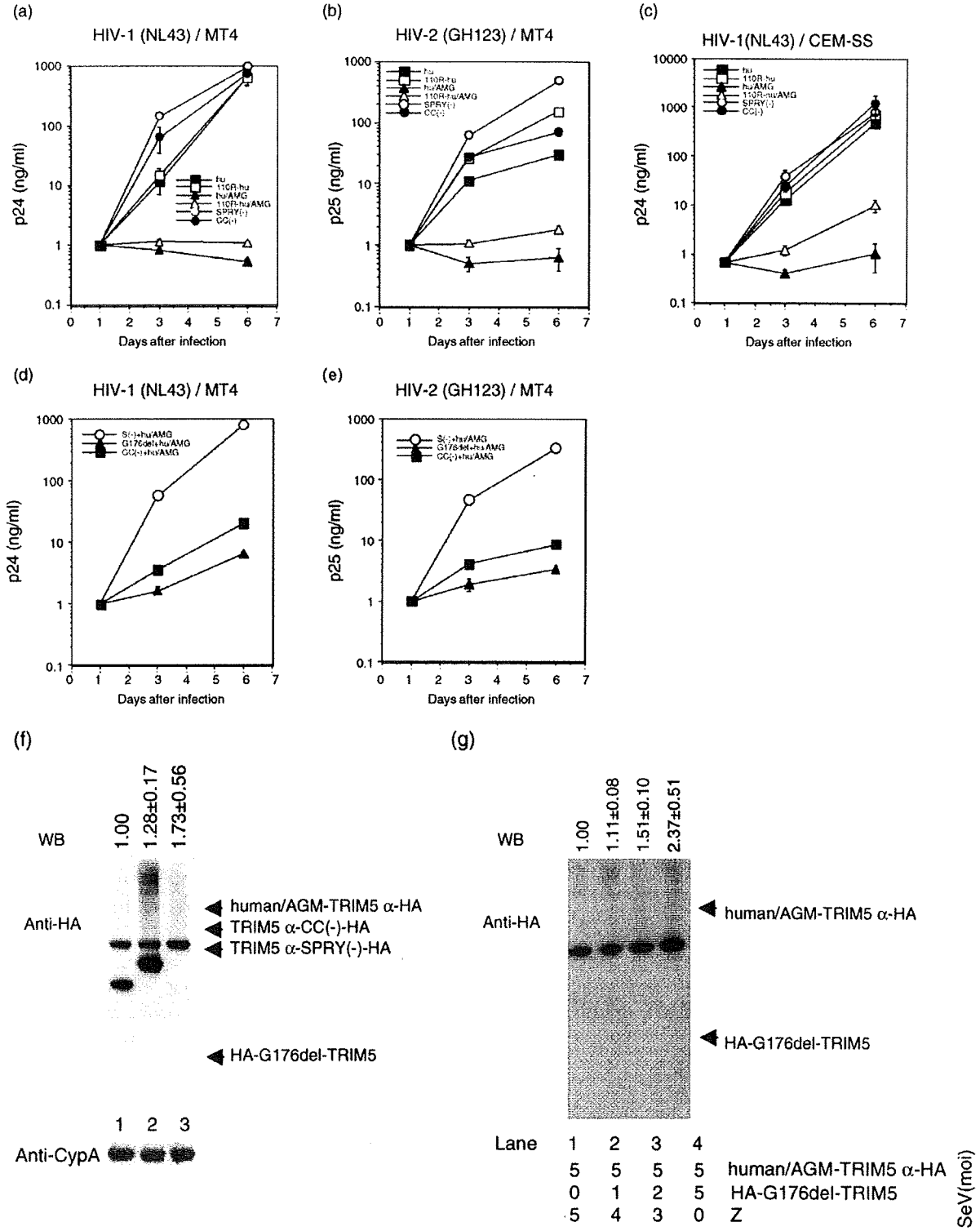

Fig. 2. Effect of TRIM5α variants on the anti-HIV-1 and anti-HIV-2 activities. Human MT4 (a, b) or CEM-SS (c) cells were infected with recombinant Sendai virus (SeV) carrying human wild-type TRIM5α (■; hu), human 110Arg-TRIM5α (□; 110R-hu), human/African green monkey (AGM) chimeric TRIM5α (▲; hu/AGM), human/AGM chimeric 110-ArgTRIM5α (△; 110R-hu/AGM), CM-TRIM5α-SPRY(−) (○; SPRY(−)) or AGM-TRIM5α-CC(−) (●; CC(−)). Nine hours after infection, cells were inoculated with HIV-1 NL43 (a and c) or HIV-2 GH123 (b). Culture surpernatants were periodically assayed for levels of p24 (a and c) or p25 (b). MT4 cells were simultaneously infected with two recombinant SeVs at 5 plaque-forming unit (PFU) per cell for

expressing dominant negative TRIM5α-SPRY(−) than in cells with noninterfering TRIM5α-CC(−), demonstrating the anti-HIV-2 activity of endogenous human TRIM5α (Fig. 2b). Both wild-type and variant human TRIM5α exhibited weak but apparent anti-HIV-2 activity, and HIV-2 grew to higher titers in cells expressing the human 110Arg-TRIM5α than in cells with the human wild-type-TRIM5α (Fig. 2b). In human/AGM chimeric version, wild-type TRIM5α completely restricted HIV-2 (Fig. 2b). In contrast, HIV-2 grew to slightly higher titers in cells expressing the human/AGM chimeric 110Arg-TRIM5α than in cells expressing the wild-type human/AGM chimeric TRIM5α (Fig. 2b). These results indicated that the Gly110Arg variant weakened the anti-HIV-1 and anti-HIV-2 activities of human TRIM5α in MT4 cells.

We recently found that the expression of TRIM5α protein introduced by SeV varied depending on cell types, that is, it was much lower in CEM-SS than in MT4 cells [25]. To evaluate the anti-HIV-1 activity of variant TRIM5α at more physiological levels of expression, we performed experiments using CEM-SS (Fig. 2c). Neither wild-type nor variant human TRIM5α exhibited anti-HIV-1 activity, probably due to the low level expression of TRIM5α in CEM-SS cells. However, HIV-1 grew to approximately 10 times higher levels in cells expressing the human/AGM chimeric 110Arg-TRIM5α than in cells with the wild-type chimeric TRIM5α, suggesting that the anti-HIV-1 activity of TRIM5α in CEM-SS cells was also reduced by the Gly110Arg substitution. Therefore, we concluded that the Gly110Arg polymorphism affected both the anti-HIV-1 and anti-HIV-2 activities of human TRIM5α.

Truncated G176del-TRIM5 enhanced antiviral activity of coexpressed TRIM5α

To express the G176del-TRIM5, we added an HA-tag at its N-terminus, because the expression of G176del-TRIM5 protein tagged with HA at the C-terminus could not be detected. Although the expression of HA-fused protein was clearly visualized by anti-HA antibody, its expression was much lower than the full-length TRIM5α (Fig. 1b). In cells infected with SeV expressing the G176del-TRIM5, HIV-2 grew to the same titers as those in cells infected with SeV expressing a nonfunctional mutant TRIM5α-CC(−), indicating that the G176del-TRIM5 lost the anti-HIV-2 activity (data not shown). We then investigated whether the G176del-TRIM5 showed any effects on the anti-HIV activity of coexpressed full-length TRIM5α, because all individuals carrying the G176del variant were in the heterozygous state. As shown in Fig. 2d and 2e, both HIV-1 and HIV-2 were restricted in cells simultaneously expressing the human/AGM chimeric TRIM5α and TRIM5α-CC(−). As expected, both HIV-1 and HIV-2 grew to high titers in cells expressing the human/AGM chimeric TRIM5α and the dominant negative mutant TRIM5α-SPRY(−) [24]. In contrast, both HIV-1 and HIV-2 were severely restricted in cells expressing the human/AGM chimeric TRIM5α and G176del-TRIM5 as compared within cells expressing the human/AGM chimeric TRIM5α and TRIM5α-CC(−). These results suggested that the G176del-TRIM5 enhanced the antiviral activity induced by the full-length TRIM5α.

Next, we investigated whether the truncated G176del-TRIM5 could affect the expression of TRIM5α. Expressions of the human/AGM chimeric TRIM5α in cells expressing either TRIM5α-SPRY(−), TRIM5α-CC(−) or G176del-TRIM5 are shown in Fig. 2f. Amount of human/AGM chimeric TRIM5α in cells coexpressing the G176del-TRIM5 was 1.7 times higher than that in cells coexpressing the TRIM5α-SPRY(−). When we infected a constant amount of SeV expressing the human/AGM TRIM5α in combination with the increasing amounts of SeV expressing the G176del TRIM5 variant, we found that the expression level of human/AGM TRIM5α was increased by the G176del TRIM5 (Fig. 2g).

Discussion

It is widely accepted that within host cells, there are restriction factors that oppose retroviral replication more effectively than the conventional arms of the immune

Fig. 2. *(continued)*
each SeV. CM-TRIM5α-SPRY(−) and human/AGM chimeric TRIM5α (○; S(−) + hu/AGM), AGM-TRIM5α-CC(−) and human/AGM chimeric TRIM5α (■; CC(−) + hu/AGM), or hemaglutinin (HA)-G176del-TRIM5 and human/AGM chimeric TRIM5α (▲; G176del + hu/AGM) were simultaneously inoculated. Nine hours after the infection, cells were superinfected with HIV-1 NL43 (d) or HIV-2 GH123 (e) and culture surpernatants were periodically assayed for levels of p24 (d) or p25 (e). The means with standard deviations of triplicate samples are shown. (f) Western blottings for TRIM5 protein and cyclophilin A from MT4 cells infected with SeV expressing the HA-tagged human/AGM chimeric TRIM5α (human/AGM-TRIM5α-HA) coexpressed with the AGM-TRIM5α-CC(−)-HA (lane 1; TRIM5α-CC(−)-HA), coexpressed with the CM-TRIM5α-SPRY(−)-HA (lane 2; TRIM5α-SPRY(−)-HA), or with the HA-G176del-TRIM5 (lane 3: HA-G176del-TRIM5). The relative amounts of human/AGM chimeric TRIM5α are shown on the top with the standard deviation of six independent samples. (g) MT4 cells were infected with SeV expressing the HA-tagged human/AGM chimeric TRIM5α coinfected with SeV expressing the HA-G176del-TRIM5 or an empty vector parental Z strain. The multiplicity of infection in each SeV is shown on the bottom. The relative amounts of human/AGM chimeric TRIM5α are shown on the top with standard deviation of triplicate samples.

system [1,2]. Because TRIM5α has crucial roles in the intracellular defense mechanisms against HIV-1 [2–4], sequence variations in TRIM5α might be associated with the susceptibility to HIV-1 infection and/or progression to AIDS. In this study, we demonstrated the association of 43Tyr-allele with the reduced susceptibility to HIV-1 infection in two ethnically distinct populations. In addition, we identified two novel rare variants, Gly110Arg and G176del, both of which had an impact on the anti-HIV-1 activity and susceptibility to HIV-1 infection.

The association of His43Tyr with the HIV-1 infection or AIDS progression has been tested in several studies, but the results were not consistent [16–20]. We found that the 43Tyr-allele was less frequent in the HIV-1-infected patients than in the ethnic-matched controls in both Japanese and Indian populations. The study sizes were not very large, but two independent ethnic populations did exhibit the same trends for the association with His43Tyr. We previously analyzed HIV-1-infected long-term nonprogressors and standard progressors in France and Japan for the TRIM5α polymorphisms and failed to find any differences in the frequency of 43Tyr-allele between these two HIV-infected groups both in France and Japan [19]. However, the allele frequency of 43Tyr in the Japanese HIV-1-infected patients we analyzed in the previous study was 0.143, which was similar to that in the present study (0.133, Table 1). Interestingly, several studies have reported that the anti-HIV-1 activity of TRIM5α with 43Tyr was lower than that with 43His [16,18]. In our previous study, we also showed that the anti-HIV-1 activity of TRIM5α with 43Tyr was lower than that with 43His, although the difference in anti-HIV-1 activity between the 43His-TRIM5α and 43Tyr-TRIM5α was very small [19]. In spite of the lower anti-HIV-1 activity of the 43Tyr-TRIM5α, several epidemiological studies have shown that the 43Tyr-allele was associated with the reduced susceptibility to HIV-1 infection [16,18], as demonstrated in this study. The reasons for the discrepancy between the epidemiological and functional effects of His43Tyr remain unclear at the moment. On the other hand, van Manen *et al.* [20] recently reported that homozygous status for 43Tyr was associated with the accelerated disease progression in white populations, which was consistent with the effect of His43Tyr variation on the anti-HIV-1 activity. Further epidemiological studies will be required to clarify the impact of His43Tyr on the susceptibility to HIV-1 infection and AIDS progression.

We also showed that the impact of His43Tyr on the susceptibility to HIV-1 infection was slightly different between Japanese and Indian. The frequency of 43Tyr-allele in the Indian HIV-1-infected patients was significantly lower than that in the Indian controls, but the significant difference was not found in Japanese. Different distribution of HIV-1 subtypes might be one of the reasons for the different contribution of 43Tyr-allele in the susceptibility, because all of the Indian patients examined in this study were infected with HIV-1 subtype C, whereas only subtype B was observed in our Japanese patients, as was found in the previous reports [26,27]. Kaumanns *et al.* [28] have reported that the antiretroviral activities of TRIM5α differed among the HIV-1 subtypes, although the differences in the in-vitro antiretroviral effect of TRIM5α between the subtypes C and B were not evident.

In this study, one focus was the functional impact of two rare TRIM5α variants found in our epidemiological studies. First, our findings indicated that the 110Arg variant weakened the anti-HIV-1 and anti-HIV-2 activities of human TRIM5α in human T-cell lines. This variant was observed more frequently in the Japanese HIV-1-infected patients than in the controls. This variation substitutes the smallest amino acid glycine with a positively charged amino acid arginine at the 110 amino acid position of TRIM5α and is located next to the amino acid residue 109Gly, which is suspected to be a zinc-coordinating residue in the B-box 2 domain [29]. This drastic change in amino acid character might change the structure of TRIM5α, in which an intact B-box 2 domain was essential for the antiretroviral activity of TRIM5α and disruption of the TRIM5α B-box domain by specific amino acid substitution resulted in loss of retroviral restriction [8,30–32]. The 3D structure of the amino acid residues 11–133 of TRIM5α was modeled by SWISS-MODEL, an Automated Comparative Protein Modeling Server (http://swissmodel.expasy.org/SWISS-MODEL.html) [33]. As shown in Fig. 3, residue 110 constituted one of the β sheets in the N-terminal half of TRIM5α. Interestingly, the location of residue 110 was close to residue 43 in the modeled 3D structure of TRIM5α (Fig. 3b and 3c). As described previously, His43Tyr was reported to affect antiretroviral activity. These data suggested that residue 110 might be one of the key amino acid residues in the TRIM5α structure like residue 43.

Second, we found that the truncated G176del-TRIM5 enhanced the antiviral activity of coexpressed full-length TRIM5α. Coinfection of SeVs expressing the G176del-TRIM5 and human/AGM-TRIM5α was accompanied by the increased protein level of full-length human/AGM-TRIM5α. The amount of human/AGM chimeric TRIM5α in cells coinfected with SeVs expressing the G176del-TRIM5 was 1.7 times higher than in cells coinfected with SeVs expressing the TRIM5α-SPRY(−). These data suggested that the truncated TRIM5α was degraded rapidly, resulting in a delay of the degradation process of full-length TRIM5α and leading to the augmentation of protein levels. Recently, we observed that coexpression of a splice variant of TRIM5, TRIM5γ, increased the amount of TRIM5α.